International Journal of Physical Sciences

Volume 9 Number 4 28 February, 2014
ISSN 1992-1950

Academic Journals

ABOUT IJPS

The **International Journal of Physical Sciences (IJPS)** is published weekly (one volume per year) by Academic Journals.

International Journal of Physical Sciences (IJPS) is an open access journal that publishes high-quality solicited and unsolicited articles, in English, in all Physics and chemistry including artificial intelligence, neural processing, nuclear and particle physics, geophysics, physics in medicine and biology, plasma physics, semiconductor science and technology, wireless and optical communications, materials science, energy and fuels, environmental science and technology, combinatorial chemistry, natural products, molecular therapeutics, geochemistry, cement and concrete research, metallurgy, crystallography and computer-aided materials design. All articles published in IJPS are peer-reviewed.

Submission of Manuscript

Submit manuscripts as e-mail attachment to the Editorial Office at: ijps@academicjournals.org. A manuscript number will be mailed to the corresponding author shortly after submission.

For all other correspondence that cannot be sent by e-mail, please contact the editorial office (at ijps@academicjournals.org).

The International Journal of Physical Sciences will only accept manuscripts submitted as e-mail attachments.

Please read the **Instructions for Authors** before submitting your manuscript. The manuscript files should be given the last name of the first author.

Editorial Board

Instructions for Author

Electronic submission of manuscripts is strongly encouraged, provided that the text, tables, and figures are included in a single Microsoft Word file (preferably in Arial font).

The **cover letter** should include the corresponding author's full address and telephone/fax numbers and should be in an e-mail message sent to the Editor, with the file, whose name should begin with the first author's surname, as an attachment.

Article Types

Three types of manuscripts may be submitted:

Regular articles: These should describe new and carefully confirmed findings, and experimental procedures should be given in sufficient detail for others to verify the work. The length of a full paper should be the minimum required to describe and interpret the work clearly.

Short Communications: A Short Communication is suitable for recording the results of complete small investigations or giving details of new models or hypotheses, innovative methods, techniques or apparatus. The style of main sections need not conform to that of full-length papers. Short communications are 2 to 4 printed pages (about 6 to 12 manuscript pages) in length.

Reviews: Submissions of reviews and perspectives covering topics of current interest are welcome and encouraged. Reviews should be concise and no longer than 4-6 printed pages (about 12 to 18 manuscript pages). Reviews are also peer-reviewed.

Review Process

All manuscripts are reviewed by an editor and members of the Editorial Board or qualified outside reviewers. Authors cannot nominate reviewers. Only reviewers randomly selected from our database with specialization in the subject area will be contacted to evaluate the manuscripts. The process will be blind review.

Decisions will be made as rapidly as possible, and the journal strives to return reviewers' comments to authors as fast as possible. The editorial board will re-review manuscripts that are accepted pending revision. It is the goal of the IJPS to publish manuscripts within weeks after submission.

Regular articles

All portions of the manuscript must be typed double-spaced and all pages numbered starting from the title page.

The Title should be a brief phrase describing the contents of the paper. The Title Page should include the authors' full names and affiliations, the name of the corresponding author along with phone, fax and E-mail information. Present addresses of authors should appear as a footnote.

The Abstract should be informative and completely self-explanatory, briefly present the topic, state the scope of the experiments, indicate significant data, and point out major findings and conclusions. The Abstract should be 100 to 200 words in length.. Complete sentences, active verbs, and the third person should be used, and the abstract should be written in the past tense. Standard nomenclature should be used and abbreviations should be avoided. No literature should be cited.

Following the abstract, about 3 to 10 key words that will provide indexing references should be listed.

A list of non-standard **Abbreviations** should be added. In general, non-standard abbreviations should be used only when the full term is very long and used often. Each abbreviation should be spelled out and introduced in parentheses the first time it is used in the text. Only recommended SI units should be used. Authors should use the solidus presentation (mg/ml). Standard abbreviations (such as ATP and DNA) need not be defined.

The Introduction should provide a clear statement of the problem, the relevant literature on the subject, and the proposed approach or solution. It should be understandable to colleagues from a broad range of scientific disciplines.

Materials and methods should be complete enough to allow experiments to be reproduced. However, only truly new procedures should be described in detail; previously published procedures should be cited, and important modifications of published procedures should be mentioned briefly. Capitalize trade names and include the manufacturer's name and address. Subheadings should be used. Methods in general use need not be described in detail.

Results should be presented with clarity and precision. The results should be written in the past tense when describing findings in the authors' experiments. Previously published findings should be written in the present tense. Results should be explained, but largely without referring to the literature. Discussion, speculation and detailed interpretation of data should not be included in the Results but should be put into the Discussion section.

The Discussion should interpret the findings in view of the results obtained in this and in past studies on this topic. State the conclusions in a few sentences at the end of the paper. The Results and Discussion sections can include subheadings, and when appropriate, both sections can be combined.

The Acknowledgments of people, grants, funds, etc should be brief.

Tables should be kept to a minimum and be designed to be as simple as possible. Tables are to be typed double-spaced throughout, including headings and footnotes. Each table should be on a separate page, numbered consecutively in Arabic numerals and supplied with a heading and a legend. Tables should be self-explanatory without reference to the text. The details of the methods used in the experiments should preferably be described in the legend instead of in the text. The same data should not be presented in both table and graph form or repeated in the text.

Figure legends should be typed in numerical order on a separate sheet. Graphics should be prepared using applications capable of generating high resolution GIF, TIFF, JPEG or Powerpoint before pasting in the Microsoft Word manuscript file. Tables should be prepared in Microsoft Word. Use Arabic numerals to designate figures and upper case letters for their parts (Figure 1). Begin each legend with a title and include sufficient description so that the figure is understandable without reading the text of the manuscript. Information given in legends should not be repeated in the text.

References: In the text, a reference identified by means of an author‘s name should be followed by the date of the reference in parentheses. When there are more than two authors, only the first author‘s name should be mentioned, followed by ’et al‘. In the event that an author cited has had two or more works published during the same year, the reference, both in the text and in the reference list, should be identified by a lower case letter like ’a‘ and ’b‘ after the date to distinguish the works.

Examples:

Abayomi (2000), Agindotan et al. (2003), (Kelebeni, 1983), (Usman and Smith, 1992), (Chege, 1998; 1987a,b; Tijani, 1993,1995), (Kumasi et al., 2001)

References should be listed at the end of the paper in alphabetical order. Articles in preparation or articles submitted for publication, unpublished observations, personal communications, etc. should not be included in the reference list but should only be mentioned in the article text (e.g., A. Kingori, University of Nairobi, Kenya, personal communication). Journal names are abbreviated according to Chemical Abstracts. Authors are fully responsible for the accuracy of the references.

Examples:

Ogunseitan OA (1998). Protein method for investigating mercuric reductase gene expression in aquatic environments. Appl. Environ. Microbiol. 64:695-702.

Gueye M, Ndoye I, Dianda M, Danso SKA, Dreyfus B (1997). Active N2 fixation in several Faidherbia albida provenances. Ar. Soil Res. Rehabil. 11:63-70.

Charnley AK (1992). Mechanisms of fungal pathogenesis in insects with particular reference to locusts. In: Lomer CJ, Prior C (eds) Biological Controls of Locusts and Grasshoppers: Proceedings of an international workshop held at Cotonou, Benin. Oxford: CAB International, pp 181-190.

Mundree SG, Farrant JM (2000). Some physiological and molecular insights into the mechanisms of desiccation tolerance in the resurrection plant Xerophyta viscasa Baker. In Cherry et al. (eds) Plant tolerance to abiotic stresses in Agriculture: Role of Genetic Engineering, Kluwer Academic Publishers, Netherlands, pp 201-222.

Short Communications

Short Communications are limited to a maximum of two figures and one table. They should present a complete study that is more limited in scope than is found in full-length papers. The items of manuscript preparation listed above apply to Short Communications with the following differences: (1) Abstracts are limited to 100 words; (2) instead of a separate Materials and Methods section, experimental procedures may be incorporated into Figure Legends and Table footnotes; (3) Results and Discussion should be combined into a single section.

Proofs and Reprints: Electronic proofs will be sent (e-mail attachment) to the corresponding author as a PDF file. Page proofs are considered to be the final version of the manuscript. With the exception of typographical or minor clerical errors, no changes will be made in the manuscript at the proof stage.

International Journal of Physical Sciences

Table of Contents: Volume 9 Number 4, 28 February, 2014

ARTICLES

academicJournals

Vol. 9(4), pp. 48-53, 28 February, 2014
DOI: 10.5897/IJPS2013.4025
ISSN 1992 - 1950

http://www.academicjournals.org/IJPS

International Journal of Physical Sciences

Full Length Research Paper

A phenomenological model for photon mass generation *in vacuo*

Masroor H. S. Bukhari[1,2]

[1]Department of Physics, University of Houston, Houston, TX77204, USA.
[2]Department of Physics, Jazan University, Gizan 22822, Jazan, Saudi Arabia.

Received 4 September 2013; Accepted 17 February, 2014

A phenomenological model is presented here arguing that photon mass is an induced effect rendered in the form of vacuum potential arising from vacuum natural modes. An elementary vacuum potential is defined as a function of vacuum zero-point fields, which yields an expression for effective photon mass generation. A Lagrangian is constructed for this model which incorporates photons with effective mass *in vacuo*. It is suggested that photons may acquire or present an effective mass while interactions with vacuum or other fields but they do not have an intrinsic rest mass. The photon mass emerges as a dynamical variable which depends on the coupling strength of electromagnetic fields to the vacuum natural modes and on the value of vector potential.

Key words: Photon mass, Maxwell-Proca equations, vacuum potentials, Higgs potential.

PACS numbers: 11, 11.15.-q, 12.10.Dm.

INTRODUCTION

There have been numerous studies in the past investigating the problem of photon mass and some comprehensive reviews (Lakes, 1998; Tu et al., 2005) on the problem can be found in literature. Photons are assumed massless as per the Standard Model of physics and Quantum Electrodynamics, however the possibility of photons with non-vanishing mass cannot be excluded. In classical formalism, photonic fields with mass are defined by the Maxwell-Proca equations (Lakes, 1998). These equations, in relativistic form, may be expressed as:

$$\partial_\mu F^{\mu\nu} + \mu^2 A^\nu = 0, \qquad \left(\mu^2 + \mu^2\right)A^\mu = 0 \tag{1}$$

Where μ is the hypothetical mass of the electromagnetic field (photon), $F_{\mu\nu}$ is electromagnetic tensor and A^μ is electric vector potential (a gauge field).

Experimentally, so far, all the searches for a significant photon mass have been negative and an upper limit of approximately 2.0×10^{-16} eV (Particle Data Book, 2012) has been set after a series of terrestrial and celestial searches. Nevertheless, photon mass problem remains an active area of physics.

It may be hypothesized that while photons remain massless gauge bosons responsible for mediating the electromagnetic interaction (as per the Standard Model), it may be possible that they can acquire or present an effective mass while undergoing interactions with other fields. In order for this to happen, the most suitable

E-mail: mbukhari@gmail.com

candidate is perhaps the vacuum and its natural mode fields, also known as zero-pint energy fields, arising from inherent fluctuations in the vacuum. It is a well-established and empirical fact that these fluctuations in vacuum lead to a number of observable effects, most importantly vacuum screening currents (Aitchison and Hey, 1982), and the Casimir force and corresponding energy (Casimir, 1948). The Casimir force and energy (in a three-dimensional plane-wave model and under absolute conditions) have a form (Casimir, 1948; Mostepenenko and Trunov, 1997).

$$F_{cas} = \frac{\hbar c \pi^2}{240} \frac{A}{L^4}$$
$$E_{cas} = \frac{\hbar c \pi^2}{720} \frac{A}{L^3} \quad (2)$$

Where A is the area of each of the two plates and L is the separation between them, and h-bar is the Planck's constant divided by 2π.

Possibility for a so-called dynamic form of the Casimir effect (Dodonov, 2010) has also been suggested in recent times. It is argued that it is possible that a mecha-nism of parametric resonance Dodonov (1996, 2010) takes place in such cases, whereby photons are created in an empty cavity by means of resonant processes, such as resonance excitation of electromagnetic modes (Dodonov, 1996; Schwinger, 1992).

Vacuum is, in its simplest form, the quantum state corres-ponding to minimum energy, with a value of constant electrical field as the amplitude of the quantum fluctuations, which designates vacuum fluctuations as real electromagnetic fields propagating in space with speed of light, like an ordinary free field. The energy of an individual zero-point field in vacuum, corresponding to the ground state (principal quantum number n=0), is expressed as:

$$E_i = \frac{1}{2}\hbar\omega \quad (3)$$

Then, the collective energy of this vacuum can be described as:

$$E_0 = \frac{1}{2}\sum_i \sqrt{\bar{p}^2 + m^2} \quad (4)$$

Planck was the first to propose, in 1911, the existence of zero-point energy associated with the black body radiation modes (Planck, 1911), with a statistical physical description. He expressed a zero-point energy superimposed onto the black-body radiation energy, giving the mean energy per mode as:

$$\bar{E} = \bar{E}_{bbr} + \frac{1}{2}\hbar\omega \quad (5)$$

Where $\bar{E}_{bbr}$ is the mean value of black body radiation.

This provides a crude estimate of the zero-point energy and length in the form of a one-dimensional harmonic oscillator formalism:

$$E_0(x) = \frac{1}{2}\sum_{\omega} \hbar\omega f(\omega),$$
$$x = \pi n/\omega \quad (6)$$

Here, a cutoff is mandatory to avoid the so-called *'vacuum catastrophe'* (Itzykson and Zuber, 1985), and f(ω) is the required cutoff function, defined as:

$$f(\omega) = 1,\ f(\omega) \xrightarrow[\omega\to\infty]{} 0 \quad (7)$$

The vacuum energy can be equated to the zero-point energy per unit volume (in discrete to continuum limits) as:

$$\langle 0|\underline{E}^2|0\rangle = \frac{1}{2\Omega}\sum_{\underline{k}s} \omega_k = \frac{1}{(2\pi)^3}\int d^3k|\underline{k}|. \quad (8)$$

The integral diverges for large frequency modes, leading to *vacuum catastrophe*, but for short frequencies, part of these fluctuating modes results in observable effects, such as the Casimir effect. After introducing the cutoff, the mean energy density for vacuum is described by summing over all filled modes up to the introduced cutoff, ω_{max}:

$$\bar{\rho}_{vac} = \frac{(\hbar\omega_{\max})^4}{8\pi^2(\hbar c)^3} \quad (9)$$

This remains valid until the cut-off frequency diverges and the density becomes infinite.

MODEL

One assumes that a massive photon field is confined within vacuum which serves as a background potential, defined here as the vacuum potential V(η), where η is a complex field;

$$V_{vac} = V(\eta) \quad (10)$$

The potential defines the energy contained in the fluctuating zero-

point fields within a physical vacuum.

Assuming a simple scalar theory, one asserts that this potential has a quartic form (which is minimum possible form in the problem at hand), and expresses this potential as follows (here the Casimir sign convention is used, otherwise negative sign is required for an attractive potential):

$$V(\eta) = \frac{1}{2}\mu^2\eta^2 + \frac{g}{2}\eta^4 \tag{11}$$

Where, g is a dimensionless coupling strength, depicting the strength of interaction of the □ field with the vacuum.

From the minimum or extreme lowest state of this potential, that is,

$$\frac{\partial}{\partial\eta}V(\eta) = 0 \tag{12}$$

One gets;

$$\frac{\partial}{\partial\eta}V(\eta) = \mu^2\eta + 2g\eta^3 = 0$$

One can calculate and see that the result yields the ground state value for the field as:

$$\eta_0 = \left(-\frac{\mu^2}{2g}\right)^{1/2}$$

$$|\eta_0| = +\left(-\frac{\mu^2}{2g}\right)^{1/2} \tag{13}$$

Then, the state of this vacuum is obtained as:

$$\eta_{vac} = \begin{pmatrix} 0 \\ . \\ . \\ \sqrt{-\frac{\mu^2}{2g}} \end{pmatrix} \tag{14}$$

The form of this vacuum is similar to the Higgs vacuum, as per the Higgs theory (Guralnik et al., 1969). The vacuum expectation value of the field is determined to be:

$$\langle\eta\rangle_0 = \langle 0|\eta|0\rangle = \begin{pmatrix} 0 \\ \eta_{vac} \end{pmatrix} \tag{15}$$

Vacuum expectation value (*vev*), $\langle 0|\eta|0\rangle$ is the non-zero equilibrium value of vacuum potential (our argument here is based upon non-perturbative aspects of vacuum). To simplify this statement, we can say that it is the macroscopic manifestation of the vacuum fluctuations, or the vacuum electromagnetic fields normal modes, which exist ubiquitously in the vacuum in an equilibrium situation, having a non-zero observable value.

Interaction of electromagnetic vector potential in this background potential has to satisfy the equation:

$$\mu A^{\mu} = \langle 0|j^{\mu}(\eta)|0\rangle \tag{16}$$

Where j^{μ} is the electromagnetic four-current associated with the potential in vacuum, expressed here as its vacuum expectation value.

Vacuum potential has to satisfy the current screening condition for massive fields, as described earlier. The screening condition becomes:

$$\langle 0|j^{\mu}(\eta)|0\rangle = -\mu^2 A^{\mu} \tag{17}$$

It is obvious that the vacuum expectation value of potential is expressed in the form of electromagnetic currents, where the screening is underlying mechanism or condition that yields an effective mass.

One can proceed to the next step and incorporate the defined vacuum potential into the Klein-Gordon equation for the massive fields (Itzykson and Zuber, 1985) obtaining:

$$(\mu^2 - \mu^2)\eta - V^2(\eta) = 0 \tag{18}$$

Now one can write down a general Lagrangian for this theory (in Adjoint representation) as:

$$L = \frac{1}{2}\partial_{\mu}\eta^a\partial_{\mu}\eta^a - \frac{1}{2}\mu^2(\eta^a\eta^a) + \frac{1}{4}g(\eta^a\eta^a)^2 \tag{19}$$

First of all, in order to incorporate the electromagnetic field, as well as to preserve gauge invariance, we introduce a specific form of the Lagrangian, called the *'Stueckelberg's Lagrangian'* (Itzykson and Zuber, 1985), and modify it to include photons with a mass μ and vector potential A_{μ} as:

$$L^{\gamma}_{em} = \frac{1}{2}\mu^2 A^a_{\mu}A^a_{\mu} - \frac{1}{4}F^a_{\mu\nu}F^a_{\mu\nu} - \frac{1}{2}(\partial\cdot A^a_{\mu})(\partial\cdot A^a_{\mu}) \tag{20}$$

and perform a covariant derivative gauge transformation:

$$\partial^{\mu} \longrightarrow D_{\mu} = \partial^{\mu}\eta^a - gc_{abc}A^b_{\mu}\eta^c \tag{21}$$

where c_{abc} are the relevant non-abelian structure constants (Frampton, 2000). With this change, the invariant electromagnetic field tensor becomes:

$$F^a_{\mu\nu} = \partial_{\mu}A^a_{\nu} - \partial_{\nu}A^a_{\mu} - gc_{abc}A^b_{\mu}A^c_{\nu} \tag{22}$$

An interaction term is required in the Lagrangian, which would depict the form of interaction between vector potential of the free electromagnetic field and the vacuum potential. This term takes the form:

$$L_{\text{int}} = \frac{1}{2}g^2(A^a_{\mu}A^a_{\mu})(\eta^a\eta^a)^2 \tag{23}$$

Here, g is the coupling strength between these two potentials or fields. But, we already have an interaction term in form of the vacuum potential we defined earlier:

$$L_{\text{int}} = V(\eta) = \frac{1}{2}\mu^2\eta^2 + \frac{g}{2}\eta^4 \tag{24}$$

On comparing the two expressions of Equations (25) and (26), one can instantly identify:

$$\frac{1}{2}\eta^2(\mu^2 + g\eta^2) = \frac{1}{2}g^2A_\mu^2\eta^2 \tag{25}$$

$$\mu^2 + g\eta^2 = g^2A_\mu^2 \tag{26}$$

Or

$$\mu^2 = g(gA_\mu^2 - \eta^2)$$
$$\mu = \sqrt{g(gA_\mu^2 - \eta^2)} \tag{27}$$

$$\mu = \sqrt{g(gA_\mu A^\mu - \eta'\eta)} \tag{28}$$

(Here $\eta'\eta$ implies η†η)

This development gives a phenomenological expression for the photon mass under the framework of this model. The mass depends on coupling strength, as expected, as well as on the vector potential (of the electromagnetic field) and the intrinsic vacuum field, η. Now substituting all the terms, we are led to the appropriate Yang-Mills (non-abelian) Lagrangian for the theory as:

$$L = \frac{1}{2}(D_\mu\eta^a)(D_\mu\eta^a) - \frac{1}{2}\mu^2\eta^a\eta^a$$
$$-\frac{1}{4}F_{\mu\nu}^aF_{\mu\nu}^a + \frac{1}{2}\mu^2A_\mu^aA_\mu^a - \frac{1}{2}(D_\mu A_\mu^a)(D_\mu A_\mu^a)$$
$$+\frac{1}{2}g(\eta^a\eta^a)^2 + \frac{1}{2}g^2(A_\mu^aA_\mu^a)(\eta^a\eta^a)^2 \tag{29}$$

Or in a simple representation:

$$L = \frac{1}{2}D_\mu\eta^2 - \frac{1}{2}\mu^2\eta^2 - \frac{1}{4}F_{\mu\nu}F^{\mu\nu} + \frac{1}{2}\mu^2A_\mu^2$$
$$-\frac{1}{2}D_\mu A_\mu^2 + \frac{1}{2}g\eta^4 + \frac{1}{2}g^2A_\mu^2\eta^4 \tag{30}$$

The first two terms define the vacuum potential η in covariant derivative form (including a mass term); the third, fourth and fifth terms depict the electromagnetic field; the sixth term represents the vacuum potential and the last term is the interaction of photons with vacuum potential. This Lagrangian defines a system of a vacuum potential interacting with enclosed electromagnetic fields, and has all the terms for the defined vacuum potential and the massive electromagnetic field, as well as their interaction.

DISCUSSION

A brief review of the origin and the form of photon mass problem has been given in the preceding sections. It is shown that photon mass arises in a simple fashion in the form of interactions between the natural modes of vacuum and the electromagnetic fields, under a gauge formalism. A possibility exists that the electromagnetic fields may interact with the vacuum modes in the form of a resonant interaction. Resonance is a well-observed phenomenon in both classical and quantum mechanics, with a myriad number of manifestations seen at both microscopic and macroscopic level systems. In quantum fields, resonance is identified and quantized in the form of a condition, the quantum mechanical resonance (QMR), wherein fields resonantly interact with each other and may result into observable effects. It is believed that the wave interactions are most efficient if they are resonant, that is, if the two or more frequencies satisfy matching conditions and the relative wave phase remains unchanged for a long time, and where in such resonant interactions, the energy conversion takes place on a much short time scale (Servin and Brodin, 2003). This is similar to other cases in quantum mechanics involving adiabatic evolution of quantum states (Lai and Ho, 1932) and in specific to the adiabatic conversion in neutrino mass generation mechanism, the so-called *MSW effect*, explained by the Mikheyev-Smirnov-Wolfenstein model (Wolfenstein, 1978). There is one more possibility for resonance to occur in these fields. This is the phenomenon of parametric resonance (Goldstein, 2002) that is, a resonance arising in an oscillating system with change of parameters, which can be applied in understanding of the vacuum and electromagnetic modes. Some ideas have been suggested in this direction in the domain of neutrino oscillations (Akhmedov, 1988), but so far a similar study in the realm of vacuum fluctuations has not been attempted.

A number of other possibilities have been alluded to the origin of photon mass. Masood (1991) has carried out a perturbative calculation for the self-mass of photon in the limit of finite-temperature and -density, in which it was suggested that the photon mass may be square of the cyclic frequency and acquired from plasma screening of photons at high frequencies. In essence, the study suggested a dynamical generation of photon mass in the form of an effective mass mechanism, rising out of the change in electromagnetic properties of certain highly dense media and resulting into modified propagator of the photon. Another possibility is suggested elsewhere (Weldon, 1982) in the case of very high-temperature backgrounds with low densities, where photons acquire dynamically-generated masses.

Finally, a conspicuous possibility for the origin of photon mass lies in the realm of gravitation, or the curvature of space-time. With the advent of Einstein's General Theory of Relativity, gravitation received a new

explanation in the form of inherent curvature of space-time near massive objects. Although efforts have been underway to find a quantum version of the theory and reconcile all the four fundamental interactions, there has been little success. The strongest evidence comes from the general theory of relativity. Recently, an experiment (Mueller, 2010) recording bending of matter waves under gravitation with high precision has further reinforced the metric nature of gravitation. Thus, it is not a far-fetched idea that just as gravitational bending of light has its origin in the space-time curvature, the same curvature can also lead to the generation of mass in electromagnetic fields.

Depending upon space-time curvature, photons can undergo interaction with gravitation. A strong evidence of this kind of interaction comes from the observed deflection of light in the proximity of heavy celestial objects (Misner et al., 1973). The bending is described in the form of a deflection angle, expressed as (Tu et al., 2005):

$$\theta = \vartheta\left(1+\frac{m_\gamma^2 c^4}{2h^2\nu^2}\right) \tag{31}$$

Where ϑ is the bending angle for photons without mass, given as;

$$\vartheta = \frac{4GM}{c^2 R} \tag{32}$$

Here, M and R are the mass and radius of the celestial object (star, quasar, black hole etc.) causing deflection and G is the Universal Gravitational Constant. Therefore, it becomes extremely important to study the behavior of photons under the influence of gravitational curvature, especially studying the effects of gravitation on the geodesic path that a photon takes.

Conclusion

Based on the foundations of existing empirical framework in quantum field theory, a model and some ideas are presented which bear potential in the study of the problem of photon mass. Ideas and formulation outlined in this paper may be summarized in the form of a few careful suggestions.

It may be suggested that the term *'rest mass'* cannot be attributed to a photon because photon is not an electrostatic concept and mass can only be ascribed to it in the form of a relativistic electrodynamic framework. Moreover, incorporating both the intrinsic properties of vacuum and the gravitational interaction are important. Mass is intrinsically a property which quantifies the quantity of matter and/or inertia in an extended object, and since the object is itself under the influence of gravitation, as defined by the general theory of relativity, it has influence from the magnitude of space-time curvature as well. It may be possible that photon (and possibly other field quanta) does not have an intrinsic mass like other fundamental particles, but in fact an effective mass, rendered to it either from the vacuum normal modes (as we saw in preceding sections) or the curvature of gravitation. This effective potential endows a proportional, observable, mass to the photon by means of an effective mass generation in the ambient vacuum or gravitational potentials.

As the mass depends on the effective potential, it does not remain a constant and in fact becomes a variable, which depends on the magnitude of potential and the interaction. In the case of vacuum, the effective mass of the photon is in fact the coupling of a photon's scalar field to the intrinsic normal modes of the vacuum, which creates an effective vacuum potential.

In the case of gravity, the effective potential of the photon mass is modified by the gravitational contributions (that is, from the gravity-induced variation in the curvature). It may possibly be a consequence of a gravitational-electromagnetic interaction of some kind as well, which has yet to be established. Serious investigations are needed on these lines.Thus, it may be possible that the interaction of photon with vacuum natural modes, either under a resonant mechanism or without resonance, can induce significant effects, including but not limited to production of photons as well as effective mass generation.

We may also surmarise that the current upper limits imposed on the photon mass may in fact be the magnitude of our best estimate on the limits of its measurement, or it may be the measurement of the limits of the effect of effective potential (attributed to the particle from the ambient vacuum potential and/or the curvature of space-time under gravity) as measured while a particular observation was carried out. It is suggested here that a more viable place to understand the origin of photon mass is in the vacuum rather than in terrestrial or celestial effects or processes which may have other influencing factors interfering with the measurement. On the basis of this study, it is summarized that photon does not have an intrinsic rest mass, however a possibility of an effective mass is not ruled out. Based upon a model presented here, the photon mass becomes a variable which depends on coupling of electromagnetic fields to vacuum modes.

ACKNOWLEDGEMENTS

Author would like to express gratitude towards Professor Ed V. Hungerford III at the Medium Energy Physics group, Department of Physics, University of Houston, for inviting me to study this interesting problem and providing

me with astute guidance and literature to initiate this study.

Conflict of Interests

The author(s) have not declared any conflict of interests.

REFERENCES

Lakes RS (1998). "Experimental limits on the photon mass and cosmic magnetic vector potential" Phys. Rev. Lett. 80:1826-1829.

Tu LC, Luo J, Gillies GT (2005). “The mass of the photon”, Rep. Prog. Phys. 68:77-130.

In Particle Data Book (2012). (Particle Data Group, Lawrence Berkeley National Laboratory, 2012); J. Beringer *et al.*, “Particle Data Book“, Phys. Rev. D. 86:1001-2526.

Aitchison IJR, Hey AJG (1982). *In Gauge Theories in Particle Physics* (Adam Hilger, Bristol) P.194.

Casimir HBG (1948). "On the attraction between two perfectly conducting plates", *Proc. K. Ned. Akad. Wet.* 51:793; K. A. Milton, *In The Casimir Effect* (World Scientific, NJ, 2001).

Mostepenenko VM, Trunov NN (1997). *In The Casimir Effect and its Applications* (Clarendon Press, Oxford, 1997), P. W. Milloni, *In The Quantum Vacuum* (Academic Press,1994).

Dodonov VV (2010). “Current status of the dynamical casimir effect”, Phys. Scr. 82:038105-038107.

Dodonov VV (1996). ”Resonance excitation and cooling in electromagnetic modes in a cavity with an oscillating wall ”, Phys. Lett. A. 213:219-225.

Schwinger J (1992). “Casimir energy for dielectrics“, Proc. Nat. Acad. Sci. 89:4091-4093.

Planck M (1911). „Eine neue Strahlungshypothese”, Verh. Deutsch. Phys. Ges. 13:138-148.

Itzykson C, Zuber JC (1985). In Quantum Field Theory. McGraw-Hill, NY. Chapter 1.

Guralnik G, Hagen CR, Kibble TWB (1969). In Advances in High-Energy Physics (Ed. By R. Cool and R. E. Marshak), Wiley, New York, 1969; R. N. Mahapatra, In Unification and Supersymmetry, Springer-Verlag, New York, 1986,1st Ed.

Frampton PH (2000). In Gauge Field Theories. John Wiley, N.Y, 2000.

Servin M, Brodin G (2003). Resonant interaction between gravitational waves, electromagnetic waves and plasma flows, Phys. Rev. D 68:44017.

Lai D, Ho WCG (1932). astro-ph/0211315 v2, Landau L. "Zur Theorie der Energieubertragung. II"., Phys. Z. Soviet Union 2(46); C. Zener, “Non-adiabatic crossing of energy levels”, Proc. R. Soc. London, Ser. A. 137:696-702.

Wolfenstein L (1978). “Neutrino oscillations in matter”, Phys. Rev. D17:2369-2374.

Goldstein H (2002). In Classical Mechanics. Addison-Wesley, NY, 2002.

Kh. Akhmedov E (1988). “Neutrino oscillations in inhomogeneous matter”, Yad. Fiz. 47:475 (1988) [Sov. J. Nucl. Phys. 47:301.

Masood SS (1991). “Photon mass in the classical limit of finite temperature and density QED”, Phys. Rev. D44:3943-3947.

Weldon HA (1982). “Covariant Calculations at Finite Temperature: the Relativistic Plasma", Phys. Rev. D26:1394-1396.

Mueller H (2010). A precision measurement of the gravitational redshift by the interference of matter waves”, P. Achim and S. Chu, Nature 463:926-928.

Misner CW, Thorn K, Wheeler JA (1973). In Gravitation. Freeman. pp. 1103-1105.

academicJournals

Vol. 9(4), pp. 54-60, 28 February, 2014
DOI: 10.5897/IJPS2013.4091
ISSN 1992 - 1950

http://www.academicjournals.org/IJPS

International Journal of Physical Sciences

Full Length Research Paper

On the nature of electric charge

Jafari Najafi, Mahdi

1730 N Lynn ST apt A35, Arlington, VA 22209 USA.

Received 10 December, 2013; Accepted 14 February, 2014

A few hundred years have passed since the discovery of electricity and electromagnetic fields, formulating them as Maxwell's equations, but the nature of an electric charge remains unknown. Why do particles with the same charge repel and opposing charges attract? Is the electric charge a primary intrinsic property of a particle? These questions cannot be answered until the nature of the electric charge is identified. The present study provides an explicit description of the gravitational constant G and the origin of electric charge will be inferred using generalized dimensional analysis.

Key words: Electric charge, gravitational constant, dimensional analysis, particle mass change.

INTRODUCTION

The universe is composed of three basic elements; mass-energy (M), length (L), and time (T). Intrinsic properties are assigned to particles, including mass, electric charge, and spin, and their effects are applied in the form of physical formulas that explicitly address physical phenomena. The meaning of some particle properties remains opaque. For example, there is no intelligible explanation of an electric charge. What is known of electric charge is its ability to generate force and an electromagnetic field and its attractive and repulsive reactions to other charged particles. It is known that an electric charge obeys the law of conservation and quantization. Constants have been identified, such as h (Planck constant), v_c (speed of light), and G (gravitational constant). Meaningful interpretations of mass-energy, length, and time in relation to these constants are also necessary. Attempts have been made to clarify the nature of electric charge, but none are comprehensive because they fail to provide explicit general formulas for the relation between electric charge and known physical parameters. The present study provides a new approach to this problem and an explicit formula that addresses the relation between electric charge and known physical parameters. This approach is of great generality and mathematical simplicity that simply and directly postulates a hypothesis for the nature of the electric charge. Although the final formula is a guesswork based on dimensional analysis of electric charges, it shows the existence of consistency between the final formula and proven physical facts.

The explanation begins with a brief introduction to dimensional analysis and how it is used. The new method is then applied to develop a formula to describe G in terms of known physical universal parameters. The new formula will be shown to be almost identical to the solution of the Friedmann equation. The guideline will be proposed to formulate an explicit definition of the nature of an electric charge. It will be shown that electric charge is equivalent to mass change in a particle. To overcome deficiencies in the new approach, the results will be compared to current proven knowledge. No contradictions or inconsistencies will be raised and excellent compatibility will be confirmed. Practically, any ambiguity in knowledge may unexpectedly produce multiple unknowns. The main purpose of this study is to eliminate obscurity about the origin of the electric charge.

E-mail: jafari001@gmail.com

DIMENSIONAL ANALYSIS

Almost all physical parameters (constants and variables) have a combination of the dimensions of mass, length, and time. The present study did not employ basic units for absolute temperature (Θ), amount of substance (N) and luminous intensity (J), and other parameters related to them. Because physical parameters are addressed, the gravitational constant and electric charge can be sufficiently expressed using a combination of M, L, and T. Constants without dimensions express values such as angle or proportions such as the ratio of particle speed to light speed. Some constants merely establish equality in the system of measurement. Some physical constants and variables do not have clear dimensions of a combination of M, L, and T. For example, the dimension of linear momentum is ML/T. This is an explicit combination of mass, length and time. The dimension of electric charge $\sqrt{4\pi\varepsilon_0 \frac{ML^3}{T^2}}$ is more complicated. The vacuum permittivity constant is ε_0, but it is not explicitly defined in terms of M, L, and T. One can easily decompose ML/T into, e.g., mass (M) and velocity of a particle (L/T), and find a formula for the linear momentum of a particle. This has not been accomplished for electric charge.

Dimensional analysis is a simple tool for understanding the relationship between physical parameters and equations based on their dimensions, but it is not used to explore and formulate unknown phenomena. It is often used to check the accuracy of calculations and equations and to express physical parameters based on their associations with other types of parameters.

The present study uses a slight generalization of this tool to find a meaningful and explicit description of the obscure physical parameter of electric charge. This method parses the dimension of an unintelligible parameter into separate parts and performs a simple mathematical manipulation on each part to convert it into a real physical parameter. Finally, the physical parameters derived for each part, keeping the final composition, will be used to present a precise definition of the relationship between the combination of M, L, and T and the original unknown parameter.

Crediting a physical parameter to a specific dimension must be based on logic and known physical facts. This method avoids any decomposition of a dimension or assigning a physical parameter to each part that promotes ambiguity in the meaning of a part. This constraint appears as a lemma that should be studied and developed. This method may not work in all cases, but gives good results for gravitational constant and electric charge.

It should be emphasized that this method and its related restrictions will not sufficiently support the final results. Each equation obtained from this method is guesswork, although dimensions for both sides of the equation are established. Experiments, measurement, and mathematical calculations based on pre-established relationships and equations confirm the conjecture; however, it is good practice to compare these results withproven physical facts.

First, the symbols [] and $[]^{-1}$ should be defined in relation to the dimensions of the physical parameters:

Definition 1: $[y] = M^{\alpha} L^{\beta} T^{\gamma}$

In this equation, $M^{\alpha} L^{\beta} T^{\gamma}$ is the dimension of physical quantity *y*. In fact, the units of any physical quantity can be expressed using a power law (Sedov, 1993).

Definition 2: $y = [M^{\alpha} L^{\beta} T^{\gamma}]^{-1}$

where a physical quantity y governs the dimension combination $M^{\alpha} L^{\beta} T^{\gamma}$.

NATURE OF THE GRAVITATIONAL CONSTANT G

Gravitational constant (G) is a constant parameter that appears in the equation of gravity:

$$F = G \frac{m_1 m_2}{r^2} \quad (1)$$

This equation itself does not provide a tangible interpretation of the nature of G. This formula does not define its source, amount, or relation to other actual parameters in the universe. To discover this relationship, the dimensions of both sides of Equation (1) for M, L and T are:

$$\frac{ML}{T^2} = [G]\frac{M^2}{L^2} \quad (2)$$

Therefore:

$$[G] = \frac{L^3}{MT^2}\frac{M}{M} \quad (3)$$

Equation (3) represents the dimension of G and states that physical parameters exist in the universe whose integration (as a formula with the above final dimension) gives the value of G. To fit this into an equation to determine the value of G in terms of physical parameters, the right side of Equation (3) is parsed into two parts and multiplied by dimensionless parameter β on the right side, obtaining:

$$G = \beta \left[\frac{L^3}{M}\right]^{-1}\left[\frac{1}{T^2}\right]^{-1} \quad (4)$$

The fraction *M/M* should not be omitted, but should

encompass in β for simplicity. This can be rewritten as:

$$G = \beta \left[\frac{4\pi/_3 L^3}{4\pi/_3 M}\right]^{-1}\left[\frac{1}{T^2}\right]^{-1} \quad (5)$$

If L is assumed to be the dimension of the radius of a sphere, the numerator of $\frac{4\pi/_3 L^3}{4\pi/_3 M}$ is the volume of that sphere:

$$G = \beta \left[\frac{V}{4\pi/_3 M}\right]^{-1}\left[\frac{1}{T^2}\right]^{-1} \quad (6)$$

Obtaining:

$$G = \frac{3}{4\pi}\beta \left[\frac{1}{\left(\frac{M}{V}\right)}\right]^{-1}\left[\frac{1}{T^2}\right]^{-1} \quad (7)$$

The mass-to-volume ratio represents the mass density (ρ). Assuming that $\frac{1}{\rho}$ and $\frac{1}{T^2}$ are real physical parameters that govern dimensions $\frac{1}{\left(\frac{M}{V}\right)}$ and $\frac{1}{T^2}$, respectively, produces:

$$G = \beta \frac{3}{4\pi\rho T^2} \quad (8)$$

Because G is a universal constant independent of any particle and reference system, the parameters of Equation (8) should be relevant to the whole universe. Therefore, let the supposed sphere be the entire universe and *M* its mass; consequently, ρ is the mass density of the universe. Also let T be the age of the universe. Now, choosing constant β gives an equation that expresses the value and nature of gravitational constant G. Regardless of the value of constant β, Equation (8) states that G is inversely proportional to the squared age and matter density of the universe. That is, if G is constant, ρ must decline steadily because of the continual increase in the value of T. Therefore, *V* (the volume of the universe) increases steadily because of the law of mass-energy conservation. Now, we compare the derived formula for G (Equation (8)), with what has been obtained, using Einstein field equations. In the matter-dominant universe, solving the Friedmann equation leads to (Komissarov, 2012):

$$G = \frac{3\Omega_m H_0^2}{8\pi\rho_m} \quad (9)$$

In this equation, the Hubble constant (H_0) is approximately the inverse of the age of universe and Ω_m is the ratio of mass density of the universe to the critical mass density. This Ω_m may be related to *M/M* in Equation (3) that was canceled and temporarily included in β.

Therefore, if we substitute β with $\frac{\Omega_m}{2}$, there will be no difference between Equations (8) and (9).

Using dimensional analysis, plus guess and intuitive analysis based on physical realities, obtains an equation to determine the physical parameters defining G. Although, this process began with a good guesswork, evaluating it using the Friedmann equation confirmed the strength of new method and correctness of its result.

NATURE OF ELECTRIC CHARGE

The question remains about the nature of electric charge and why there is no comprehensible interpretation of electric charge based on M, L and T, or a combination of known parameters of particles, such as spin and velocity. It is not known why same-charged particles repel and oppositely-charged particles attract or if electric charge is really an intrinsic property of a particle. The complicated dimension of electric charge $\sqrt{4\pi\varepsilon_0\frac{ML^3}{T^2}}$ makes it difficult to accept it as an intrinsic property of particles, when compared with simple and explicit properties like mass and spin.

Electric charge seems to be an abstract of other basic properties and physical constants. If this is true, how can an electric charge and electromagnetic field be directly measured and formulated? The answer is that the style that mass-space-time exerts its characteristic of the primary intrinsic property (related to the electric charge) leads to an observable, measurable, and summarized physical parameter known as electric charge. The reason that the main intrinsic property cannot be identified is that value is beyond current accurate measurement. It must be emphasized that this study does not refute current knowledge on electric charges and electromagnetic fields. Electric charge is certainly a known, observable, and measurable parameter of the universe. Accepted knowledge, especially Maxwell's equations, that has been subjected to countless experimentation based on the current definition of electric charge is definitely correct; however, it is necessary to overcome the obscurity about the nature of electric charge. Physics currently face unresolved problems and opened line research on the subjects such as the unified field theory, baryon asymmetry, and magnetic monopoles (Christianto et al., 2007). Defining the nature of an electric charge may also shed light on these unknown areas in physics.

Previous attempts to find the origin of electric charge include work by Shpenkov and Kreidik (2004), who developed a hypothesis based on new definition of elementary particles and their exchange in the matter-space-time field. Their theory that an electric charge is a mass change rate seems to be consistent with the results of the present study. Shpenkov (“What the Electric Charge is”) stated, "The erroneous form of the Coulomb

law gave rise to a phenomenological system of notions with measures having fractional powers of base units that are really senseless. Cognition of the nature of electric charges has become impossible". This notion is the opposite of the conclusion of this study.

Olah (2009) proposed a hypothesis that is in contrast with the current proven model of electric charges and fields. It is difficult to accept such theories. Tiwari (2006) suggested the origin of an electric charge in terms of fractional spin. Sasso (On Primary Physical Transformations of Elementary Particles: the Origin of Electric Charge) proposed a hypothesis based on relation between electric charge and spin. Nguyen (2013) discussed the change in electron charge in an external magnetic field. He stated: "the variability (or the constancy) of the mass and the electric charge of the electron still remains as a foundational problem in modern physics, awaiting to be justified". Krasnoholovets (2003) and McArthur (1999) also discussed this.

None of these works provides an explicit formula for the exact value and the nature of electric charge based on proven facts. There are two remarkable points among these discussions: there is a possible relation between electric charge and mass change, and variability of electric charge is possible. The strength of the new approach is: (1) it utilizes current proven physical equations to develop a solution; (2) a simple novel method of dimension analysis is proposed; and (3) an explicit formula for an electric charge is provided. No previously mentioned research encompasses all three benefits. A new theory is not proposed, but a different way of looking at previous hypotheses is advanced.

Using the successful dimensional analysis from the previous section, the same procedure is followed to discover the nature of electric charge beginning with Coulomb's law:

$$F = \frac{q_1 q_2}{4\pi\varepsilon_0 r^2} \tag{10}$$

Replacing the dimensions of the parameters leads to:

$$[q^2] = 4\pi\varepsilon_0 \frac{ML^3}{T^2} \tag{11}$$

Assuming dimensionless parameter (γ) and multiplying it by the right side of Equation (11) produces the following:

$$q^2 = 4\gamma\pi\varepsilon_0 [\frac{ML^3}{T^2}]^{-1} \tag{12}$$

Up to this point, the equation represents the dimension of electric charge. It also states that there must be physical parameters and constants that are integrated as a formula (with this final dimension) that equals q. The next point is to assign meaningful parameters to the components of the q dimension, beginning by decomposing $\frac{ML^3}{T^2}$. Clearly, $\frac{ML^3}{T^2}$ can be categorized in different ways using parameters with proper and valid physical interpretations. One solution is:

$$[\frac{ML^3}{T^2}]^{-1} = [\frac{ML^2}{T}]^{-1} [\frac{L}{T}]^{-1} \tag{13}$$

In this equation, $\frac{ML^2}{T}$ is the dimension of angular momentum, and $\frac{L}{T}$ is the dimension of linear velocity. Since q is the intrinsic property of the particle, angular momentum should be interpreted as particle spin. It is known that particles with non-zero spin have zero electric charge (such as electron-neutrinos). This inconsistency is troubling. In addition, in Equation (12), the roots of the parameters of angular momentum and linear velocity describe electric charge, but the root of the parameters is senseless and physically meaningless. Guesswork in this method should not conflict with known principles, although the dimension relationship is true. Slight manipulation of Equation (12) produces:

$$q^2 = 3\gamma\varepsilon_0 [\frac{4\pi L^3}{3M}]^{-1} [\frac{M^2}{T^2}]^{-1} \tag{14}$$

As in Equations (5) and (6):

$$q^2 = 3\gamma\varepsilon_0 [\frac{1}{(\frac{M}{V})}]^{-1} [\frac{M^2}{T^2}]^{-1} \tag{15}$$

Producing:

$$q^2 = 3\gamma\varepsilon_0 [\frac{1}{\rho}]^{-1} [\frac{M^2}{T^2}]^{-1} \tag{16}$$

In this equation, ρ (mass density) should be interpreted as the ρ of the particle, or a known ρ. The former produces the same problem mentioned above, which is that the root of ρ is a meaningless physical parameter. If the ρ of space is considered to be where the particle is (e.g. mass density of the universe), the problem is resolved. Using Equation (8) in Equation (16) produces:

$$q^2 = (4\pi\varepsilon_0 \alpha G T^2) [\frac{M^2}{T^2}]^{-1} \tag{17}$$

By applying final guess that governs $\frac{dm}{dt}$ to $\frac{M}{T}$ dimension produces:

$$q = \sqrt{4\pi\varepsilon_0 \alpha G}\, T \frac{dm}{dt} \tag{18}$$

In this equation, α is a dimensionless parameter and is currently unknown; T is the age of universe; $\frac{dm}{dt}$ is the mass change in the particle over time (in the particle reference frame), and q is the electric charge. Here, $\frac{dm}{dt}$ was chosen to govern $\frac{M}{T}$ because it is more pertinent,

simple and meaningful physical parameter.

Of the possible solutions for Equation (12), Equation (18) is unique and the most consistent with current proven facts and principles. When using this approach, it should be noted an independent formula for q was not proposed, but is concluded from existing formulas. Briefly, Equation (18) is an abstract of the law of gravity, Newton's 2nd law, Coulomb's law and the Freidmann equation.

Equation (18) says that the origin of an electric charge is the particle (rest-) mass change over time. In other words, mass creates a field of gravity and its change creates another field (electromagnetic). This is a surprising result because charged particles such as electrons and protons are inherently mass-variable; however, if $\left|\frac{dm}{dt}\right|$ (absolute value of $\frac{dm}{dt}$) is minuscule, it does not conflict with current proven facts. Note that Equation (18) establishes a two-way relationship between mass change and electric charge that any mass change (over time) in a particle (or physical system) will produce an electric charge (and electric field). The exact value of $\left|\frac{dm}{dt}\right|$will be given based on experimentation to determine the exact value of α. It is possible to estimate values α and $\left|\frac{dm}{dt}\right|$(for electrons), but should be kept in mind that they are not conclusive. Suppose there are two electrons separated by distance r (m). Equation (1) gives:

$$F_g = G\,\frac{m_e^2}{r^2} \tag{19}$$

where m_e is electron mass, and F_g is the gravitational force exerted on the two electrons. Equations (10) and (18) give:

$$F_e = \alpha G\, T^2\,\frac{\left|\frac{dm_e}{dt}\right|^2}{r^2} \tag{20}$$

Ratio $\frac{F_e}{F_g}$ is calculated as:

$$\frac{F_e}{F_g} = \alpha\, T^2\,\frac{\left|\frac{dm_e}{dt}\right|^2}{m_e^2} \tag{21}$$

If $\frac{F_e}{F_g}$ is alternately calculated using Equations (1) and (10), it produces:

$$\frac{F_e}{F_g} = \frac{1}{4\pi G\varepsilon_0} \times \frac{q_e^2}{m_e^2} \tag{22}$$

If the current values of Equation (22) are substituted:

$$\varepsilon_0 = 8.854 \times 10^{-12}\ Fm^{-1}$$
$$G = 6.674 \times 10^{-11}\ \ m^3\, kg^{-1} sec^{-2}$$
$$q_e = -1.602 \times 10^{-19}\ \text{coulomb}$$
$$m_e = 9.109 \times 10^{-31}\ kg$$

This gives the following for the electron:

$$\frac{F_e}{F_g}(electron) = 4.165 \times 10^{42}$$

Equation (21) has two unknown parameters, α and $\left|\frac{dm_e}{dt}\right|$. Supposing $\frac{F_e}{F_g}(electron) = \alpha$, then $\left|\frac{dm_e}{dt}\right|$ will be:

$$\left|\frac{dm_e}{dt}\right| = \frac{m_e}{T} \tag{23}$$

Substituting the values in Equation (23) or Equation (18), gives:

$$T = 4.350 \times 10^{17}\ sec$$
$$\left|\frac{dm_e}{dt}\right| = 2.094 \times 10^{-48}\ \ kg/sec$$

With the proposed assumptions and estimations, the value of $\left|\frac{dm_e}{dt}\right|$ is outside of the apparatus accuracy range. The exact value of m_e is:

$$m_e = 9.10938291\,(40) \times 10^{-31}\ kg$$

Its relative standard uncertainty is 4.4×10^{-8}. Using the value calculated for $\left|\frac{dm_e}{dt}\right|$, it takes $10^9\ sec$ (~ 30 years) for a change to occur in the least significant digit of m_e.

Using the above assumptions and calculations that summarized in Equation (23), Equation (18) may be written as:

$$q = \left(\frac{e}{m_e}\right) T\frac{dm}{dt} \tag{24}$$

where $\frac{e}{m_e}$ is a well known physical constant (although e and m_e are both time variable) that can be directly measured by experimentation. Experimental or mathematical confirmation of Equation (18) produces the following results:

(i) A change in particle mass is the source of the electric charge and electric field. A charged particle keeps its structure during mass change. There is a definite threshold for mass change in each particle; thereafter, the particle decays or annihilates.

(ii) A change in particle mass increases or decreases, making the electric charge positive or negative.

(iii) It is necessary to investigate how the mass of a

charged particle changes and the role of photon particles in this process. Two overall scenarios exist: (1) mass (energy) exchange directly between charged particles; (2) mass (energy) exchange independently between each charged particle and space. In any case, the mass of negatively charged particle increases and, for positively-charged particles, it decreases, regarding Equation (24). A justification for attractive and repulsive characteristics of charged particles must be found based on their mass change.

(iv) If $\left|\frac{dm}{dt}\right|$ is constant, for each charged particle:

$$m_0(t) = \pm \left|\frac{dm}{dt}\right| \times t + m_0(t=0) \quad (25)$$

where t is the age of the particle, m_0 is the rest mass of the particle, $m_0(t=0)$ is the initial mass of the particle and $t=0$ is the time at which the particle began to act as a charged particle (continuous mass change).

(v) If $\left|\frac{dm}{dt}\right|$ is constant, then $\frac{d^2m}{dt^2}$ will be zero, since:

$$T = t + \tau \; ; \; \tau \geq 0 \quad (26)$$

where T is the age of universe, t is the age of the charged particle; thus, τ is the difference between them. Equation (18) gives:

$$\frac{dq}{dt} = \pm \sqrt{4\pi\varepsilon_0 \alpha G}\left|\frac{dm}{dt}\right| \; C/sec \quad (27)$$

where $\frac{dq}{dt}$ is constant and non-zero for all charged particles. Because the magnetic field is proportional to $I = \frac{dq}{dt}$, this means that charged particles necessarily create the magnetic field (Biot-Savart law). Today, it is believed that there is inherent magnetism in charged particles such as electrons. This agrees with the proposed conclusion.

There is currently no approved experiment or mathematical calculation that directly assesses the conjecture about the nature of electric charge, but the present results do not create any contradiction with current knowledge about the electric charge and its effects. The validity of the results is supported by the law of gravity, Newton's 2nd law, Coulomb's law and the Freidmann equation.

DISCUSSION

Utilizing dimensional analysis to govern physical parameters to combinations of basic dimensions to identify unknown physical phenomena provides weaker mathematical support for the derived equation. This is the inherent deficiency of the approach. To overcome this deficiency, two further steps should be taken; comparing the final result with known and proved physical facts and conducting experiments to directly evaluate the results. This section compares the proposed hypothesis on the nature of electric charge with proven facts.

(a) The possibility of a charged particle without mass continues to be advanced by some parties. A similar question arises in the Reissner-Nordstrom solution of Einstein's field equations. The Reissner-Nordstrom metric (for a black hole with mass M and charge q) is:

$$ds^2 = \left(1 - \frac{r_s}{r} + \frac{r_q^2}{r^2}\right)dt^2 - \left(1 - \frac{r_s}{r} + \frac{r_q^2}{r^2}\right)^{-1} dr^2 - r^2 d\theta^2 - r^2 \sin^2\theta \; d\varphi^2 \quad (28)$$

where $r_s = \frac{2GM}{c^2}$ (Schwarzschild radius) and $r_q^2 = \frac{Gq^2}{4\pi\varepsilon_0 c^4}$. It is possible to show that it is physically impossible to make the mass M in the Reissner-Nordstrom solution vanish, because the charge itself generates an electromagnetic mass that is part of M or constitutes all of mass M. The electromagnetic mass vanishes only when the charge vanishes (Pekeris, 1982). In agreement with this result, in Equation (18), the electric charge will be zero; if the mass of particle is constant (zero or nonzero value), and electric charge exists if and only if the mass of the particle is variable (and definitely exists). However, there is no restriction for the mass of a charged particle to become zero instantaneously. Ibohal and Kapil (Charged black holes in Vaidya backgrounds: Hawking's Radiation, Department of Mathematics, Manipur University, India) discussed a similar case for the Reissner-Nordstrom solution.

(b) It is more realistic to consider the Reissner-Nordstrom metric for a black hole in a non-flat background Friedman-Robertson-Walker universe. It can be shown that the mass and charge of the black hole both vary with the evolution of the universe (Chang and Shuang, 2004; Ibohal, 2002). The variability of mass and charge of charged particles is the pivotal result of Equation (18).

(c) The influence of cosmological expansion on local systems is still a subject of research. Some authors support the view that cosmic expansion affects only systems larger than a certain spatial scale and that there is no effect below that scale. Others believe that all systems are subject to the effect of cosmic expansion, although this effect is numerically negligible for small systems (like atoms) and stronger for larger objects. This expands the validity of the Friedmann-Lemaitre-Robertson-Walker metric down to small scale (Bochicchio et al., 2013; Jose J. Arenas: The effect of the cosmological expansion on local systems: Post-Newtonian approximation). In Equation (18), factor T is $\frac{1}{H_0}$ (where H_0 is the Hubble constant). This result strongly supports the latter idea and vice versa.

(d) Based on Equation (18), particles have an absolute equal electric charge if and only if they have an equal $\left|\frac{dm}{dt}\right|$. Thus, the amount of electric charge is independent of the amount of mass. This has been seen for charged particles, such as electron and proton, yet it continues to be expected that charge is dependent on mass (e.g. mass change).
(e) All stars, black holes, and planets experience eras during which they experience mass-energy exchange with space. According to Equation (18), all of them should be considered to be charged particles for this period. Thus, they have an electromagnetic field surrounding them. This was proven in nature of electric charge.
(f) Equation (18) states that charged particles with decreasing mass (e.g., positive charge) have finite life times because of their finite mass; thus, charged particles are not fundamentally stable. This provides a good explanation of proton decay as proposed by GUTs and is still a matter of subject and observation (Senjanovi´c, 2009).
(g) Experiments show that electric charge is quantized; the q of every charged particle is an integer multiple of elementary charge e. Equation (24) clearly shows that each charged particle is a multiple of e, although it cannot singly guarantees that the coefficient is integral.

This discussion shows the excellent consistency of Equation (18) with currently-accepted physical facts. It sufficiently supports the hypothesis offered herein to describe the nature of electric charge, and adequately eliminates the weakness of the method applied to formulate the electric charge in terms of known physical parameters.

CONCLUSION

This study introduced a generalization of dimensional analysis of the physical equations and parameters and utilized this method to identify an explicit relation between gravitational constant G, and two universe parameters (age and mass density). Also, It was found that the origin of an electric charge (and electromagnetic field) is mass change of particle(s) over time. Therefore, mass change should be considered as the primary intrinsic property of charged particle rather than electric charge. It is a surprising result that, if experimentally or mathematically proven, will significantly influences some areas of physics and our view of the universe. It appears that dimensional analysis is not only a reliable method for assessing the validity of equations, but also it can help to find a meaningful interpretation for a category of unknown physical parameters. This method effectively uses speculation and intuition that is founded on proven facts and logic.

Conflict of Interests

The author(s) have not declared any conflict of interests.

REFERENCES

Arenas JJ (2013). The effect of the cosmological expansion on local systems: Post-Newtonian approximation. arXiv:1309.3503 [gr-qc].
Bochicchio I, Faraoni V (2013). Cosmological expansion and local systems: A Lemaˆıtre-Tolman-Bondi model. arXiv:1111.5266v3 [gr-qc].
Chang JG, Shuang NZ (2004). Reissner-Nordstr¨om Metric in the Friedman- Robertson-Walker Universe. arXiv:gr-qc/0407045v2.
Christianto V, Smarandache F (2007). Thirty Unsolved Problems in the Physics of Elementary Particles. Progress Phys. 4:112-114.
Ibohal Ng (2002). On the variably-charged black holes in general relativity: Hawking's radiation and naked singularities. Class. Quantum Grav. 19 4327 doi:10.1088/0264-9381/19/16/308.
Komissarov SS (2012). Cosmology. Lecture, Room: 10.19 in Maths Satellite, email: S.S.Komissarov@leeds.ac.uk.
Krasnoholovets V (2003). On the nature of the electric charge, Hadronic J. Supplement 18(4):425-456.
McArthur W (1999). The Nature of Electric Charge, the general science journal.
Nguyen HV (2013). A Foundational Problem in Physics: Mass versus Electric Charge.
Olah S (2009), The Electric Charge**,** *Copyright © 2009, the general science journal*.
Pekeris CL (1982). Gravitational field of a charged mass point. Proc. NatL Acad. Sci. USA, 79:6404-6408.
Sedov LI (1993). Similarity and dimensional methods in mechanics. 10th edn. CRC Press, Boca Raton.
Senjanovi´c G (2009). Proton decay and grand unification. arXiv:0912.5375v1 [hep-ph].
Shpenkov GP, Kreidik LG (2004). Dynamic Model of Elementary Particles and Fundamental Interactions. *GED* Special Issues, GED-East, pp. 23-29.
Tiwari SC (2006). The Nature of Electronic Charge.Foundations of Physics Letters, 1(19):51-62.

academicJournals

Vol. 9(4), pp. 61-70, 28 February, 2014
DOI: 10.5897/IJPS2013.4074
ISSN 1992 - 1950

http://www.academicjournals.org/IJPS

International Journal of Physical Sciences

Full Length Research Paper

A model for removing sediments from open channels

Hassan A. Omran[1], Mohammed Y. Fattah[1]* and Sadiq Q. Sulaiman[2]

[1]Building and Construction Engineering Department, University of Technology, Baghdad, Iraq.
[2]Civil Engineering Department, University of Al-Anbar, Iraq.

Received 18 November, 2013; Accepted 14 February, 2014

The problems caused by suspended sediment overloading in open channels are of great importance to the hydraulic engineers. One of the important problems caused by the sediment overloading during flood seasons is the change in bed level and corresponding water level of rivers due to its deposition on the river bed. At the upstream reaches, the bed slope is high, velocity is high and hence the rivers carry large amount of sediment during flood seasons. In this paper, eighty-one experiments on a laboratory open-channel of cross-section dimensions (20*50) cm and (10) m long. The experiments include using sharp crested weir in the last third part of the channel. Three heights of weir are used; namely half width of channel (B), equal to the width, and 1.5 times the width of channel). Also, three bed slopes of the channel are used; namely 0.015, 0.0225, and 0.03). In all experiments, the values of discharge are limited between 100 and 300 l/min. The concentration of suspended sediment is measured upstream and downstream the weir through each experiment to calculate the sediment reduction ratio (SRR%). The results of the laboratory experiments showed that the sediment reduction ratio increases with the increase of weir height and reaches about (63%) at a channel bed slope of (0.015) and a weir height 1.5B. When the discharge is more than (100 l/min), the highest values of sediment reduction ratio are obtained for the three slopes used and at weir height of 1.5B.

Key words: Open channel, sediment reduction ratio, model, removal.

INTRODUCTION

Many hydraulic engineering projects concern the control of sedimentation. For some large engineering projects, such as construction of a navigation channel over many kilometers in a shallow estuary, comprehensive control of sedimentation is extremely costly.

Slope–channel coupling and in-channel sediment storage can be important factors that influence sediment delivery through catchments. Sediment budgets offer an appropriate means to assess the role of these factors by quantifying the various components in the catchment sediment transfer system.

When a sediment beach covered by stones or an armor layer is exposed to breaking waves, the turbulence generated by the breaking waves can cause mobilization and removal of the sediment underneath the stones.

Sedimentation in dams, rivers, estuaries, and coastal regions has important environmental and economic influences. Different researchers studied the sediment transport and control in open channels. Zhu et al. (1999) presented an optimal–control model of sedimentation. The model contains the determination of optimal location and scheduling of dredging to minimize the total cost and

*Corresponding author. E-mail: myf_1968@yahoo.com.

to obtain a channel where water depths are not less than specified values. The system governing equations which were used in the model are:

$$\frac{\partial \vec{v}}{\partial t} + \vec{v}.\nabla v + f(k.\vec{v}) = -g.\nabla z + A.\nabla \vec{v} - C_D \frac{\vec{v}}{h} ----- \quad (1)$$

$$\frac{\partial h}{\partial t} + \nabla(\vec{v}.h) = 0 ---------- \quad (2)$$

$$\frac{\partial h.S}{\partial t} + \nabla(\vec{v}h.S) = \zeta\nabla(h\nabla S) + \alpha w(S' - S) ---- \quad (3)$$

where: $\vec{v}$ = Depth-averaged velocity in continuous governing equation, k = Empirical constant, h = Water depth in governing continuous equations, S = Sediment mass mixed rate in continuous governing equations, S' = Sediment carrying ability of water flow, t = Time step, C_D = Drag coefficient, ζ = Diffusion coefficient of sediment, w = Falling speed of sediment particle, and α = Empirical coefficient.

Barkdoll and Ettema (1999) determined the limits to which submerged vanes can be used in preventing excessive bed-sediment ingestion into lateral diversions of flow from alluvial channels, by a laboratory flume experiments. The experiments showed that a scheme of submerged vanes placed at the diversion entrance admits only a negligible rate of bed-sediment entry into the diversion when the ratio of unit discharge in the diversion to that in the main channel is less than about 0.2. Beyond this value, the effectiveness of the vanes diminishes.

Nino (2002) developed a simple theory to account for the observed downstream variation of the median sediment size in Chilean rivers based on a reach-wise equilibrium sediment transport concept. The theory make use of a bed load transport equation, linked with a resistance equation to estimate the median sediment diameter as a function of channel slope with the flow Reynolds number and bed load concentration as parameters. The formulas which were used in this research are Meyer-Peter, Muller's, Ackers and White's formulas:

$$\frac{q_s}{\sqrt{gRd_s^3}} = 8(\tau_* - \tau_{*_c})^{3/2} -------- \quad (4)$$

where: q_s = Bed load transport rate, R = Sediment submerge specific density, d_s = Sediment size, τ_* = Dimensionless bed shear stress, τ_{*_c} = Threshold dimensionless value of bed shear stress, and g = Acceleration of gravity.

The resulting model was validated against field data corresponding to 150 rivers in Central Chile, covering slopes in the range of 0.04 to 8.61% with median sediment size in the range of 0.3 to 250 mm.

Theoretical analysis

The erosion, deposition, and transport of sediment by water arise in a variety of situations with engineering implications. Erosion must be considered in the design of stable channels or the design for local scour around bridge piers. Re-suspension of possibly contaminated bottom sediments has consequences for water quality. Deposition is often undesirable since it may hinder the operation, or shorten the working life, of hydraulic structures or navigational channels. Sediment traps are specifically designed to promote the deposition of suspended material to minimize their downstream impact, e.g., on cooling water inlet works, or in water treatment plants. A large literature exists on approaches to problems involving sediment transport; the following can only introduce the basic concepts in summary fashion.

It is oriented primarily to applications in steady uniform flows in a sand-bed channel; problems involving flow non-uniformity, unsteadiness, and gravel-beds, are only briefly mentioned and coastal processes are treated in the section on coastal engineering. Cohesive sediments for which physic-chemical attractive forces may lead to the aggregation of particles are not considered at all. The finer fractions (clays and silts) that are susceptible to aggregation are found more in estuarial and coastal shelf regions rather than in streams (Lyn, 2003).

The characteristics of sediment

Density, size, and shape

The exact shape of a sediment particle is not spherical, and so a compact specification of its geometry or size is not feasible. Two practical measures of grain size are: (i) the *sedimentation or aerodynamic diameter* — the diameter of the sphere of the same material with the same fall velocity, *ws* , under the same conditions, and (ii) the *sieve diameter* — the length of a side of the square sieve opening through which the particle will just pass. Because size determination is most often performed with sieves, the available data for sediment size usually refer to the sieve diameter, which is taken to be the geometric mean of the adjacent sieve meshes, that is, the mesh size through which the particle has passed, and the mesh size at which the particle is retained. The sedimentation diameter is related empirically to the sieve diameter by means of a *shape factor,* S.F., which increases from 0 to 1 as the particle becomes more spherical (for well-worn sand, S.F. ≈ 0.7).

Size distribution

Naturally occurring sediment samples exhibit a range of grain diameters. A characteristic diameter, *da*, may be defined in terms of the percent, *a* by weight of the sample that is smaller than *da*. Thus, for a sample with d_{84} = 0.35 mm, 84% by weight of the sample is less than 0.35 mm in diameter. The *median* size is denoted as d_{50}.

Fall (or settling) velocity

The *terminal velocity* of a particle falling alone through a stagnant fluid of infinite extent is called its fall or settling velocity, w_s. The standard drag curve for a spherical particle provides a relationship between *d* and *w*.

Angle of repose

The *angle of repose* of a sediment particle is important in describing the initiation of its motion and hence sediment erosion of an inclined surface, such as a stream bank. It is defined as the angle, q, at which the particle is just in equilibrium with respect to sliding due to gravitational forces.

Sediment transport

Three modes of sediment transport are distinguished: *wash load, suspended load,* and *bed load*. Wash load refers to very fine suspended material, e.g., silt, that because of their very small fall velocities, interacts little with the bed. It will not be further considered since it is determined by upstream supply conditions rather than by local hydraulic parameters. Suspended load refers to material that is transported downstream primarily in suspension far from the bed, but which because of sedimentation and turbulent mixing still interacts significantly with the bed. Finally, bed load refers to material that remains generally close to the bed in the bedload region, being transported mainly through rolling or in short hops (termed saltation). The relative importance of the two modes of sediment transport may be roughly inferred from the ratio of settling velocity to shear velocity, w_s/u^*. For $w_s/u^* < 0.5$, suspended load transport is likely dominant, while for $w_s/u^* > 1.5$, bedload transport is likely dominant.

Measurement of sediment transport

In addition to, and contributing to, the difficulties in describing and predicting accurately sediment transport, total load measurements, particularly in the field are associated with much uncertainty. Natural alluvial channels may exhibit a high degree of spatial and temporal nonuniformities, which are not specifically considered in the 'averaged' models discussed above.

Standard methods of suspended load measurements in streams include the use of depth-integrating samplers that collect a continuous sample as they are lowered at a constant rate (depending on stream velocity) into the stream, and the use of point integrating samplers that incorporate a valve mechanism to restrict sampling, if desired, to selected points or intervals in the water column. Such sampling assumes that the sampler is aligned with a dominant flow direction, and that the velocity at the sampler intake is equal to the stream velocity.

In the vicinity of a dune-covered bed, these conditions cannot be fulfilled. The finite size of the suspended load samplers implies that they cannot measure the bedload discharge, which must therefore be measured with a different sampler or estimated with a bedload model.

The study of Cheng and Chiew (1998) presented a theoretical derivation for a new pickup probability formulation for sediment transport. Sand particles were assumed to be subjected to a hydraulically rough flow. The derived equation compares well with the experimental data found in published literature. Using the proposed relation, the Shields criterion for the definition of the threshold condition for sediment transport is equivalent to 0.6% of the pickup probability.

Results from five physical hydraulic model studies of riverside water intakes situated along the Missouri River reach between Sioux City, Iowa, and St. Louis, Missouri were presented by Nakato and Ogden (1998). Movable-bed, undistorted Froude-scale models were used to determine the effectiveness of structural modifications in the vicinity of the intake to limit the influx of bed-load sediments. Solutions developed in each case included a series of submerged flow-turning vanes located on the riverward side of the intake. A sediment-barrier wall between the vanes and intake increases the stream wise velocity component, enhancing the effectiveness of flow-turning vanes in maintaining a deep scour trench. Effective solutions determined using physical hydraulic models were verified at the prototype scale, as demonstrated by years of trouble-free operation at locations where the recommended sediment-control measures have been installed. Results presented provided design guidelines for bed load sediment control at riverside water-intake structures on sand-bed rivers.

Although, a one-dimensional (1D) mathematical model based on the nonequilibrium transport of sediment is rational in principle, its application to rivers requires empirical determination of a key coefficient in the basic equation of transport, and this is known as the adjustment coefficient. It also requires, as all ID models do, empirical and rather arbitrary apportioning of the computed total scour or deposition to the wetted perimeter. An attempt was made by Zhou and Lin (1998)

to avoid both. The equation of sediment transport was written for a vertical stream tube of infinitesimal width for which the adjustment coefficient has been rationally determined. A procedure of lateral integration was then applied to obtain the global values of the said coefficient for the entire cross section and the distribution of deposition/erosion to the wetted perimeter. The shape of the cross section is thus determined along with the amount of deposition/erosion. Results obtained with this model compare favorably with those of depth-integrated two-dimensional (2D) computations and physical model testing, both carried out for the dam neighborhood of the Three Gorges Project.

An optimal-control approach was presented by Zhu et al. (1999). It determines optimal locations and scheduling of dredging to minimize total cost and to obtain a channel where water depths are not less than specified values. The optimal-control problem is formulated and a method was developed. The optimization problem was solved by the conjugate gradient method, and the gradient of the cost function was calculated by solving the adjoint problem. A simulation study was conducted using a 2D numerical model to demonstrate the method.

Barkdoll and Ettema (1999) presented the findings of laboratory flume experiments conducted to determine the limits to which submerged vanes can be used in preventing excessive bed-sediment ingestion into lateral diversions of flow from alluvial channels. The experiments showed that a scheme of submerged vanes placed at the diversion entrance admits only a negligible rate of bed-sediment entry into the diversion when the ratio of unit discharge in the diversion to unit discharge in the main channel, q_r, is less than about 0.2. Beyond this value, the effectiveness of the vanes diminishes. The sediment-control performance of the vanes can be enhanced in several ways. One enhancement is the use of a skimming wall in conjunction with the vanes. The wall and the vanes are effective for values of q_r up to about 0.3. Another enhancement was to widen the diversion entrance such that, at the entrance, q_r does not exceed about 0.3. Further potential enhancements (modified vane shape, uniformity of flow distribution into the diversion, and increased flow velocity into the diversion) were found not to be effective. The findings are supported by observations of flow and bed-sediment behavior at a flume-scale diversion.

Sumer et al. (2001) presented the results of an experimental investigation on suction removal of sediment from between armor blocks/stones placed on a loose bed. The process of suction has been investigated. It was found that the vortices that form in the holes between the armor blocks are key to the process. The sediment swept into these vortices is entrained into the main body of the flow by these same vortices (the suction removal of sediment from between the armor blocks). The critical condition for the onset of suction was determined. It was found that the onset of suction is governed by two parameters: (1) the Shields parameter (based on the sediment size); and (2) the ratio of sediment size to stone size, d/D.

The stability of randomly deposited sediment beds was examined by McEwan and Heald (2001) using a discrete particle model in which individual grains are represented by spheres. The results indicated that the threshold shear stress for flat beds consisting of cohesionless uniformly sized grains cannot be adequately described by a single-valued parameter; rather, it is best represented by a distribution of values. Physically, this result stems from the localized heterogeneity in the arrangement of surface grains. For uniformly sized beds, geometric similarity exists such that the critical entrainment shear stress distributions scale directly with grain size. A Shields parameter of 0.06 is commonly used to define ‘‘threshold conditions,’’ and it was found that this corresponds to a point on the distributions where approximately 1.4% by weight of the surface is mobile.

A simple theory was developed by Nino (2002) to account for the observed downstream variation of the median sediment size in Chilean rivers based on a reach-wise equilibrium sediment transport concept. The theory makes use of a bedload transport equation linked with a resistance equation to estimate the median sediment diameter as a function of channel slope, with the flow Reynolds number and bedload concentration as parameters. Both, Meyer-Peter and Mu¨ller’s and Ackers and White’s formulas are used alternatively as bedload equations. A Manning–Strickler type of formulation was used as a resistance relationship. The resulting model was validated against field data corresponding to 150 rivers in Central Chile, covering slopes in the range of 0.04 to 8.61%, with median sediment size in the range of 0.3 to 250 mm. Despite the simplicity of the theory and the somewhat bold assumptions made in its derivation, the estimated variation of the median sediment size with channel slope follows the same trend as the field data. Most of the scatter of these data falls within the theoretical limits given by the estimated range of values of the parameters of the model.

Experimental results on sediment removal efficiency of vortex chamber type sediment extractors were reported by Athar et al. (2002). A geometric configuration of the extractor was identified that is able to remove even the fine sediment ($0.055 < d < 0.22$ mm) from flow with high efficiency. For the purpose of analysis, the experimental data of present study were compiled with the data from other laboratories and the field that were collected previously by other investigators. Since the existing relations were not found to produce satisfactory results, a new relationship was developed for determination of the sediment removal efficiency of the vortex chamber type sediment extractors.

A steady, two-dimensional numerical model was created by Naser et al. (2005) to study the hydrodynamics of a rectangular sedimentation basin

a **b**

Figure 1. Open channel used in the experiments.

under turbulent conditions. The strip integral method was used to formulate the flow equations, using a forward marching scheme for solving the governing partial differential equations of continuity, momentum, advection–diffusion, turbulent kinetic energy, and its dissipation. In this way the flow equations were converted to a set of ordinary differential equations in terms of the key physical parameters. These parameters, along with a set of shape functions, describe flow variables including the velocity, the concentration of suspended sediments, and both the kinetic energy and its dissipation rate. Four Gaussian distributions were investigated, one corresponding to each flow parameter. In order to calculate the turbulent shear stresses, a two-equation turbulence model (that is, k-ε model) was used. A fourth order Runge–Kutta method numerically integrates the set of ODEs. Simulation results were compared with experimental data, and close agreement (generally within 5 to 10%) was observed.

Gopakumar and Jesuraj (2012) dealt with development of a new mathematical model to simulate non-equilibrium transport of suspended sediment in open channels, with special emphasis on sediment overloading. Equilibrium transport of bed sediment was also included. Sources of the suspended sediment were from the catchment (such as construction sites, mining areas etc.). This sediment was brought into rivers and canals by flowing rainwater.

Its overloading can result in large changes in bed and water levels of the rivers and also in heavy silting of the canal beds. A new mathematical model to simulate this effect was derived based on the control volume approach. The model was tested using data available in literature and results were found satisfactory. The developed model was then applied to a hypothetical flood and sediment routing problem in a river and analyses of the results were given.

The objective of the present study is to build a small scale open channel model and study the effect of some parameters on sedimentation. These parameters include channel width, bed slope and flow discharge.

Laboratory works

In the present work, eighty-one experiments on the laboratory open-channel of cross-section dimensions (20*50) cm and (10) m long as shown in Figure 1. Each test was repeated three times and the average value for sediment concentration was calculated. The experiments included using sharp crested weir in the last third part of the channel. Three heights of weir were used; namely half width of channel (B), equal to the width, and 1.5 times the width of channel. Also, three bed slopes of the channel are used; namely 0.015, 0.0225, and 0.03.

In all experiments, the values of discharge are limited between 100 and 300 l/min. The concentration of suspended sediment was measured upstream and downstream the weir through each experiment to calculate the sediment reduction ratio (SRR%) as follows:

$$SRR\% = \frac{S_{us} - S_{ds}}{S_{us}} * 100 \text{ - - - - -} \quad (5)$$

where: S_{us} = Suspended sediment concentration upstream weir, and S_{ds} = Suspended sediment concentration downstream weir.

The water used in the experiments was taken from the Euphrates river at Al-Ramadi city west of Iraq.

ANALYSIS OF RESULTS AND DISCUSSION

Three variables are studied in this research which are the weir height, the slope of channel bed, and the discharge. To study their effect on the efficiency of weir in sediment

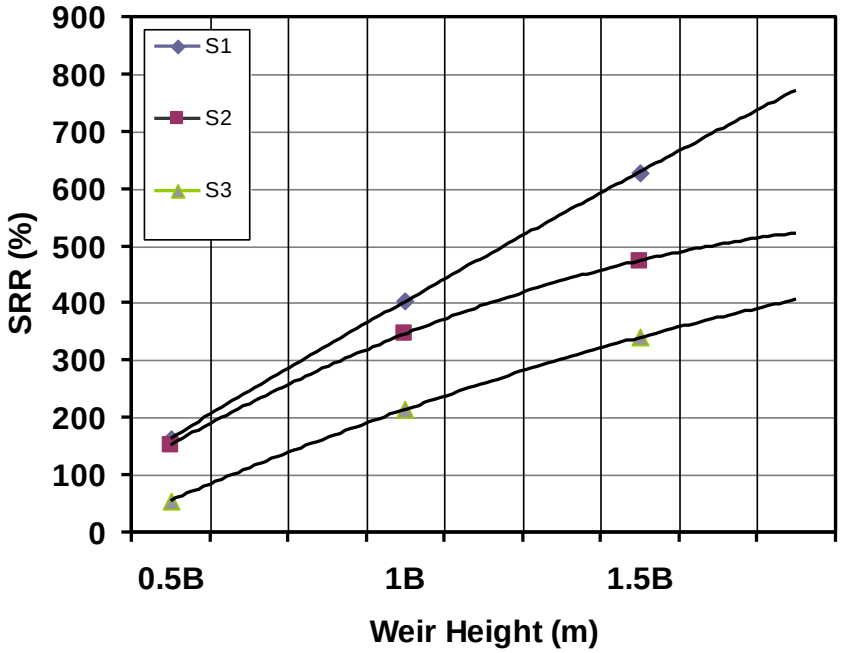

Figure 2. Variation of sediment reduction ratio with weir height for different slopes of the channel, discharge = 100 l/min.

removal, the sediment reduction ratio (SRR%) is measured. It was noted that (SRR%) increases with the increase of weir height, but decreases while the channel bed slope increases as shown in Figure 2. The figure shows that (SRR%) reaches about (63%) at channel bed slope (0.015) and weir height (1.5B) where (B) is the width of channel.

The results coincide with the principles of hydraulics of flow which state that with increasing the slope of the channel bed, the flow velocity increases which causes to lift the particles through water depth and reduce the probability of sediment trapping. The figure shows also that (SRR%) increases with increasing of the weir height due to the same reason.

The results for other values of discharge revealed the same relations shown in Figure 2 for discharge (100 l/min) and these results are illustrated in Figures 3 and 4 for a discharge value of 200 and 300 l/min, respectively.

Figures 5, 6 and 7 show the variation of (SRR%) with the discharge for three channel bed slopes and weir heights. It is noted that when the discharge is greater than (100 l/min), the highest values of (SRR%) are obtained for the three slopes and at weir height (1.5B) as shown in Figure 5. The figures also show that the differences between the values of (SRR%) for discharges (100 l/min) and (200 l/min) are not significant, then the (300 l/min) is the discharge suitable to provide acceptable (SRR%).

This can be attributed to that the initial motion of a sediment particle occurs when the ratio of the hydrodynamic force to the submerged weight force acting on the particle exceeds a certain limit determined by the geometry of the particle and the particle Reynolds number.

In Figure 8, the variation of sediment reduction ratio is drawn with discharge for different heights of weir. The figure shows that (SSR%) increases slightly with the increase of discharge. For the first slope (0.015), the increasing in discharge causes a little increase in flow velocity and the difference is converted into cross section flow area. Then, the difference in (SRR%) for the two values of discharge; 200 and 300 l/min is slightly small, the value of discharge of 300 l/min is suitable to give considerable (SRR%) for all weir heights. The role of fluid discharge approves that the sedimentation process must consider both the characteristics of the sediment and the fluid motion as was stated by Naser et al. (2005).

The same trend of variation of (SRR%) with discharge is observed in Figures 9 and 10, but the values of SRR decrease with the increase of the channel bed slope because the increase of bed slope leads to increase the flow velocity more than the cross sectional area of flow.

This behavior can be understood since the relevant sediment characteristics are not only the settling velocities of the individual particles but also whether they retain their individualities as they settle. When two particles of a nonflocculent material come together, the only effect is the momentary mutual interference; if two particles of flocculent material interact they combine into a new particle with different properties. Thus, during the sedimentation of nonflocculent materials, the sediment characteristics are constant, while the characteristics of

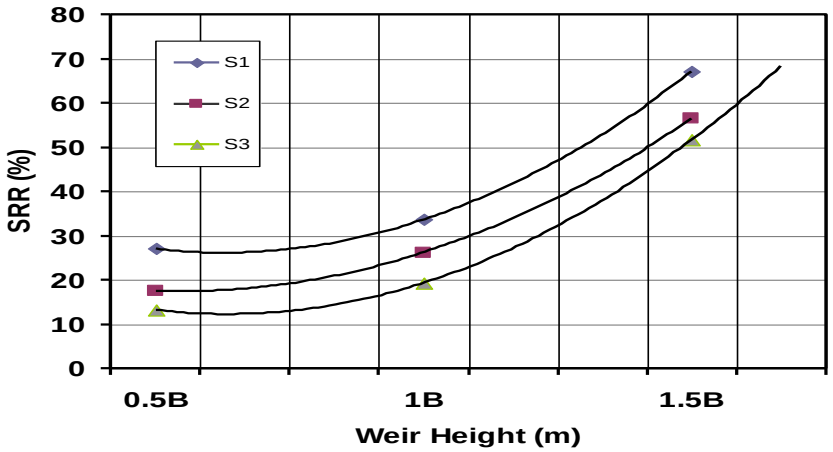

Figure 3. Variation of sediment reduction ratio with weir height for different slopes of the channel, discharge = 200 l/min.

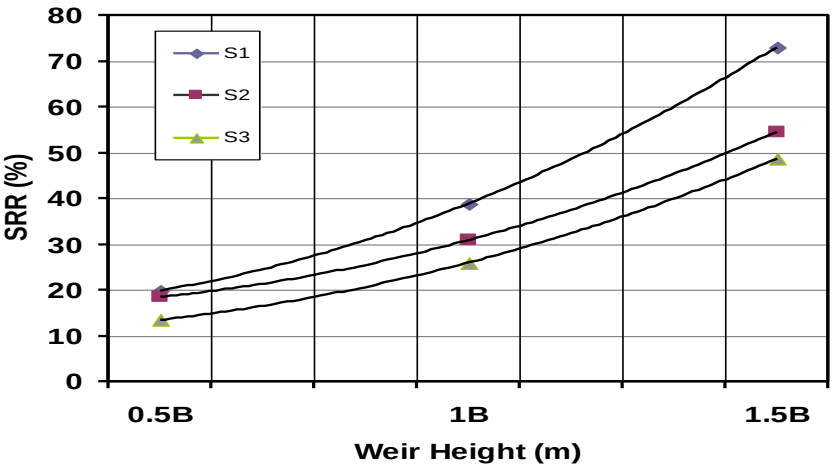

Figure 4. Variation of sediment reduction ratio with weir height for different slopes of the channel, discharge = 300 l/min.

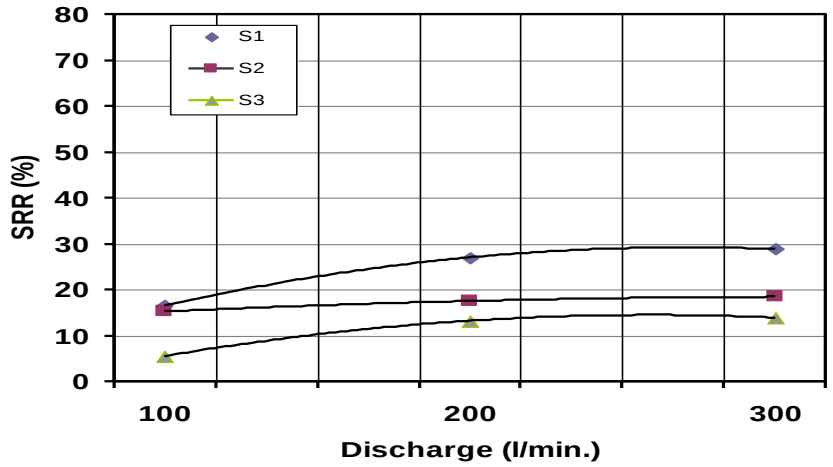

Figure 5. Variation of sediment reduction ratio with discharge for different slopes of the channel, H = 0.5 B.

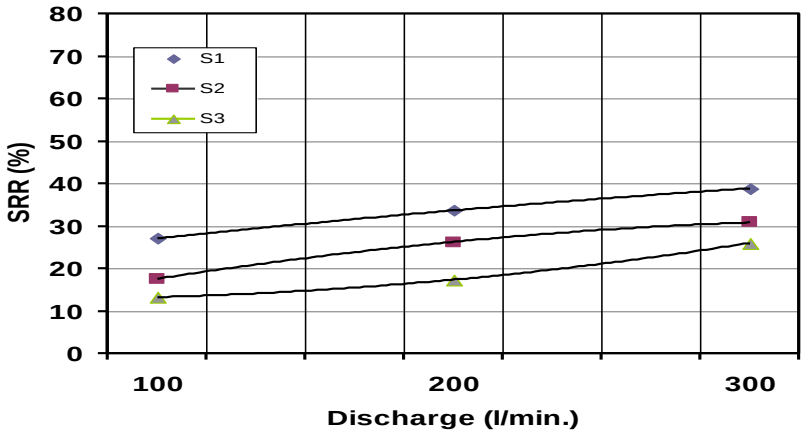

Figure 6. Variation of sediment reduction ratio with discharge for different slopes of the channel, H = B.

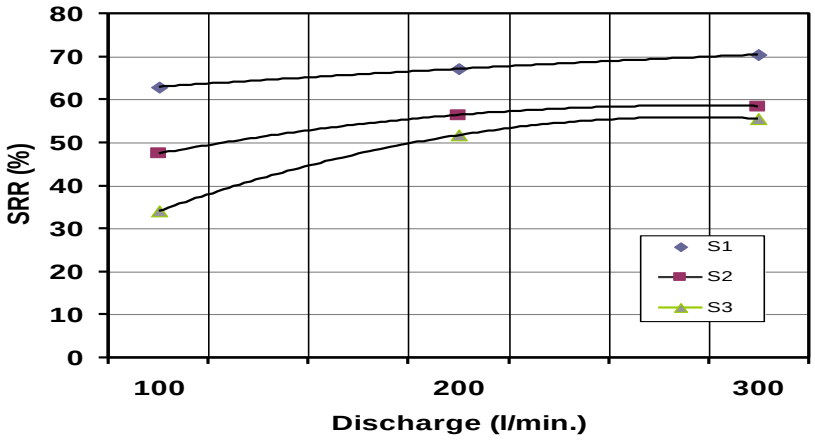

Figure 7. Variation of sediment reduction ratio with discharge for different slopes of the channel, H = 1.5 B.

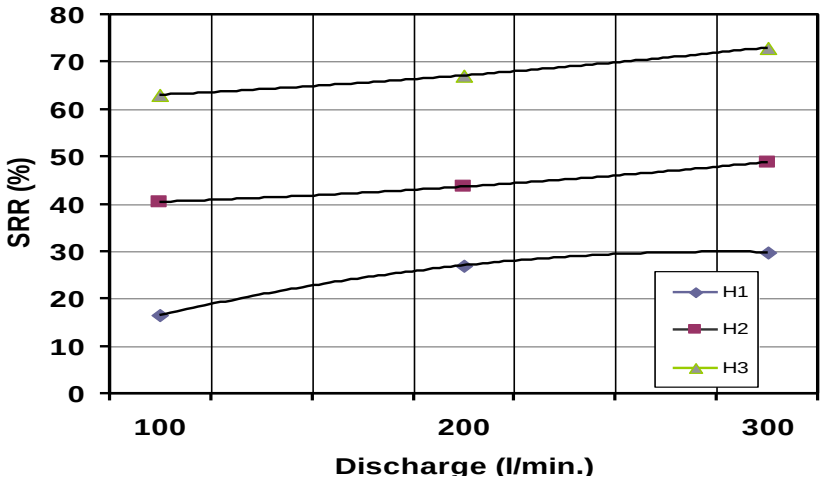

Figure 8. Variation of sediment reduction ratio with discharge for weir heights of the channel, slope S_1.

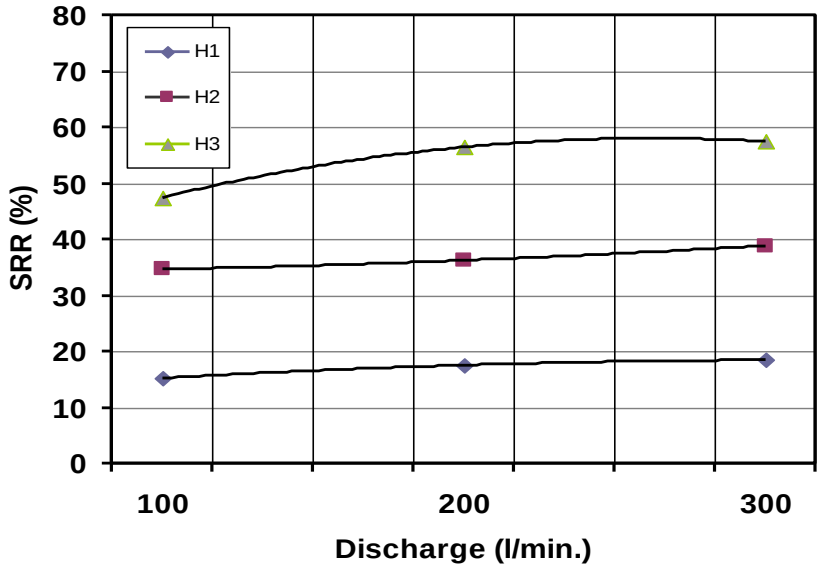

Figure 9. Variation of sediment reduction ratio with discharge for weir heights of the channel, slope S_2.

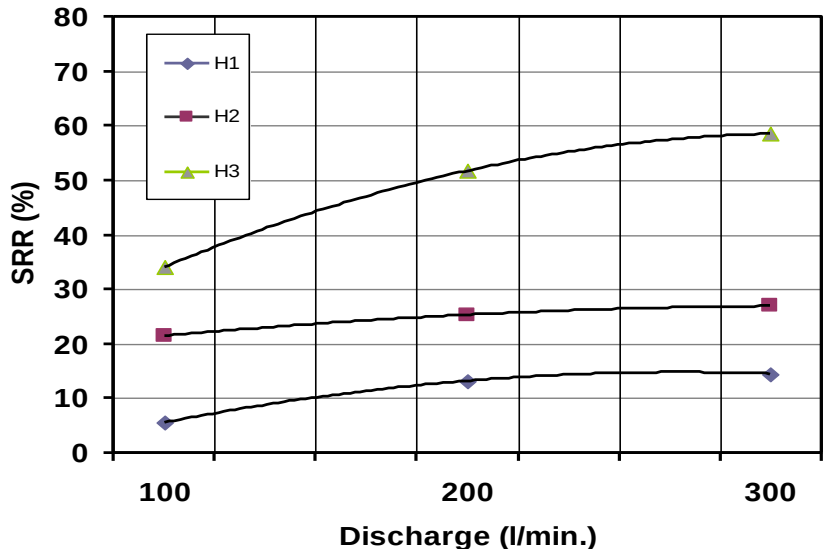

Figure 10. Variation of sediment reduction ratio with discharge for weir heights of the channel, slope S_3.

flocculent materials change continuously in a way that depends on both the sediment and flow characteristics (Naser et al., 2005).

Conclusions

Three variables were studied in this research which are the weir height, the slope of channel bed, and the discharge. Studying their effect on the efficiency removal of sediments leads to the following conclusions:

1. The sediment reduction ratio increases with the increase of weir height and reaches about (63%) at a channel bed slope of (0.015) and a weir height of 1.5B (where B is the width of channel).
2. When the discharge is more than (100 l/min), the highest values of sediment reduction ratio are obtained

for the three slopes used and at a weir height of 1.5B.
3. The value of discharge (300 l/min) is suitable to provide a considerable sediment reduction ratio for all weir heights.

Conflict of Interests

The author(s) have not declared any conflict of interests.

REFERENCES

Athar M, Kothyari UC, Garde RJ (2002). Sediment Removal Efficiency of Vortex Chamber Type Sediment Extractor, J. Hydraulic Eng, ASCE, 128(12):1051-1059.

Barkdoll BD, Ettema R (1999). Sediment Control at Lateral Diversions: Limits and Enhancements to Vane Use, J. Hydraulic Eng. ASCE, 125(8):862-870.

Cheng NS, Chiew YM (1998). Pickup Probability for Sediment Entrainment, J. Hydraulic Eng. ASCE, 124(2):232-235.

Gopakumar R, Jesuraj R (2012). Simulation of Non-Equilibrium Transport of Suspended Sediment in Open Channels, Int. J. Soft Comput. Eng. (IJSCE), 2(5):57-61.

Lyn DA (2003). Sediment Transport in Open Channels, in the “Civil Engineering Handbook”, edited by WF CHEN, JY. Richard, Lie W, second edition, 2003, CRC PRESS.

McEwan I, Heald J (2001). Discrete Particle Modeling of Entrainment from Flat Uniformly Sized Sediment Beds, J. Hydraulic Eng. ASCE, 127(7):588-597.

Nakato T, Ogden FL (1998). Sediment Control at Water Intakes along Sand-Bed Rivers, J. Hydr. Eng. ASCE, 124(6):589-5996.

Naser Gh, Karney BW, Salehi AA (2005). Two-Dimensional Simulation Model of Sediment Removal and Flow in Rectangular Sedimentation Basin, J. Environ. Eng. ASCE, 131(12):1740-1749.

Nino Y (2002). Simple Model for Downstream Variation of Median Sediment Size in Chilean Rivers, J. Hydr. Eng. ASCE, 128(10):934-941.

Sumer BM, Cokgor S, Fredsøe J (2001). Suction Removal of Sediment from Between Armor Blocks, J. Hydr. Eng. ASCE, 127(4):293-306.

Zhou J, Lin B (1998). One -Dimensional Mathematical Model for Suspended Sediment by Lateral Int. J. Hydraulic Eng. ASCE, 124(7):712-717.

Zhu J, Zeng Q, Guo D, Liu Z (1999). "Optimal Control of Sedimentation in Navigation Channels, J. Hydr. Eng. ASCE, 125(7):750-759.

academicJournals

Vol. 9(4), pp. 71-78, 28 February, 2014
DOI: 10.5897/IJPS2013.4078
ISSN 1992 - 1950

http://www.academicjournals.org/IJPS

International Journal of Physical Sciences

Full Length Research Paper

Lehmann Type II weighted Weibull distribution

N. I. Badmus[1]*, T. A. Bamiduro[2] and S. G. Ogunobi[3]

[1]Department of Statistics, Abraham Adesanya Polytechnic, Ijebu-Igbo, Nigeria.
[2]Department of Mathematical Sciences, Redeemer's University, Redemption Camp, Ogun State, Nigeria.
[3]Department of Science Laboratory Tehnology, Abraham Adesanya Polytechnic, Ijebu-Igbo, Nigeria.

Accepted 5 February, 2014

We upgrade on the method used on weighted Weibull model proposed by Azzalini (1985) using the logit of Beta function by Jones (2004) to have Lehmann Type II weighted Weibull model with a view to obtaining a distribution that is more better than both weighted Weibull and Weibull distribution in terms of estimate of their characteristics and their parameter. The weighted Weibull distribution is proposed by slightly modifying the method of Azzalini (1985) on weighted distribution with additional shape (β) and scale (λ) parameters. Some basic properties of the newly proposed distribution including moments and moment generating function, survival rate function, hazard rate function, asymptotic behaviours, and the estimation of parameters have been studied.

Key words: Asymptotic, hazard rate, Lehmann Type II, moments, weighted-Weibull.

INTRODUCTION

The Weibull distribution is a well known common distribution and has been a powerful probability distribution in reliability analysis, while weighted distributions are used to adjust the probabilities of the events as observed and recorded. The Weibull distribution can also be used as an alternative to Gamma and Log-normal distribution in reliability engineering and life testing. Numerous authors/researchers have been worked on Weibull and exponential distribution in literature. In a nut shell, Shahbaz et al. (2010) applied Azzalini's method with the Weibull distribution that produced a new class of weighted Weibull distribution in which they obtained the probability density and cumulative density function as given below:

$$f(x) = \frac{\alpha+1}{\alpha}\lambda\beta x^{\beta-1}e^{-\lambda x^{\beta}}\left(1 - e^{-\alpha\lambda x^{\beta}}\right); \quad \alpha, \beta, \lambda, \; x > 0 \quad (1)$$

The graph of the probability density function of Equation (1) with $\alpha = 4, \beta = 3$ is given Figure 1.

$$F(x) = \frac{\alpha+1}{\alpha}\left[\left(1 - e^{-\lambda x^{\beta}}\right) - \frac{1}{\alpha+1}\left(1 - e^{-(1+\alpha)x^{\beta}}\right)\right] \quad (2)$$

In the literature, researchers/authors on Lehmann Type II are very few. Figure 1 is the pdf graph of the weighted Weibull by Shabarz (2010). The aim of this article is to introduce this distribution and study on its statistical properties. This article presents the proposed distribution Lehmann Type II weighted Weibull distribution. Thereafter, moments and moment generating function is studied. This is followed by a critical discussion of the estimation of parameters showing the empirical distribution of data and the study was concluded.

*Corresponding author. E-mail: idowuolasunkanmi8169@yahoo.com

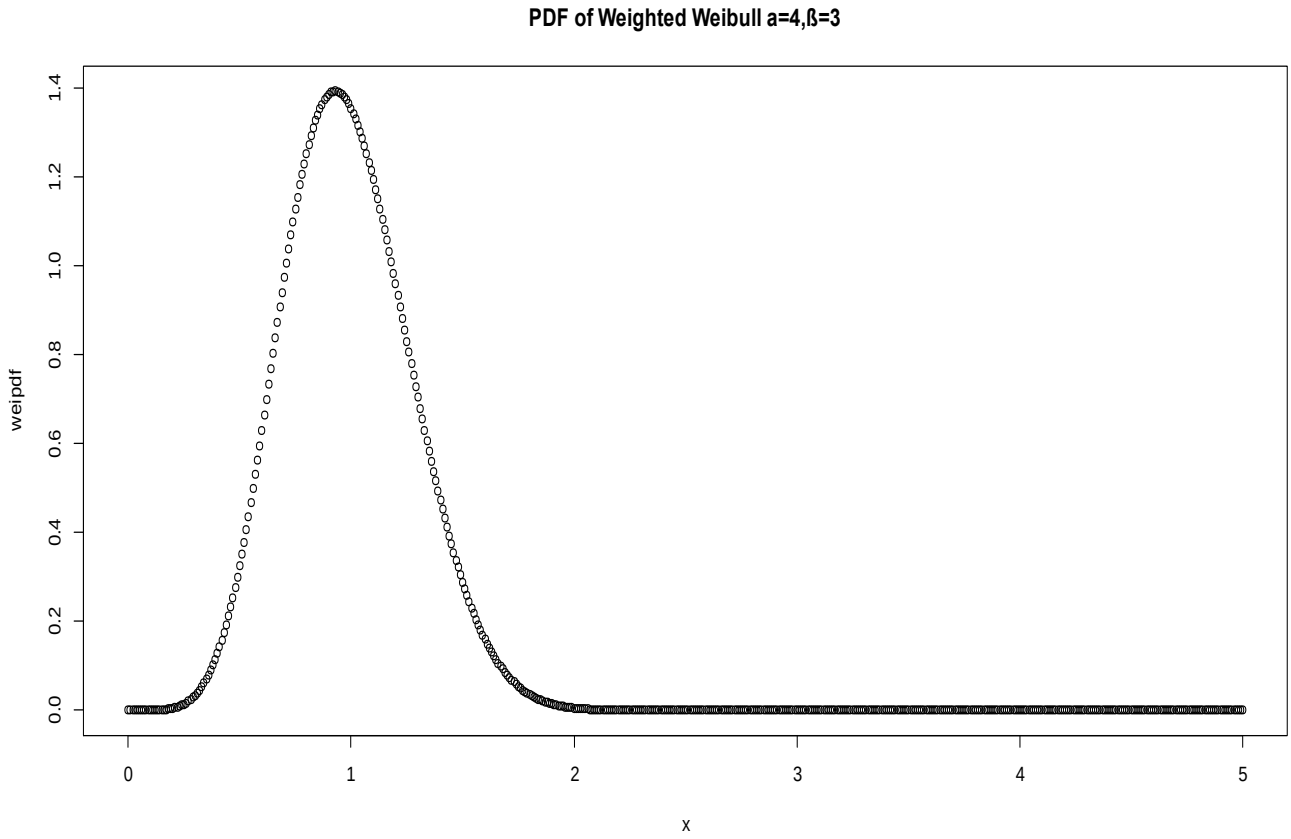

Figure 1. The probability density function of weighted Weibull distribution with $\alpha = 4, \beta = 3$ and the cumulative density function from Equation (1) is given in Equation (2).

MATERIALS AND METHODS

The proposed Lehmann Type Ii weighted Weibull distribution

The logit of beta function (the link function of the beta generalized distribution) is introduced by Jones (2004), since then extensive work has been done using the logit of beta distribution in literature. For instance, Gupta and Kundu (1990) proposed a generalized exponential distribution that provides an alternative to exponential and Weibull distribution. Lee et al. (2007), Eugene and Famoye (2002) and Nadarajah and Kotz (2005) also used the logit of beta distribution and they provided an extension on exponential distribution. The logit of beta distribution used by Famoye and Olugbenga (2005) to introduce the Beta-Weibull distribution alongside its major properties. The transformation $Exp^c F$ is called the Lehmann Type I distribution. There is a dual transformation defined by $Exp^c(1-F)$ referred to as the Lehmann Type II distribution introduced by Cordeiro et al. (2011) among others. Figures 2, 3 and 4 shows pdf, cdf and hazard rate graphs at several values of parameters. Figure 2 clearly shows that it is rightly skewed, Figure 3 rise upward to right and Figure 4 shows the level at which the hazard rate by rightly upward breaking points.

Now, let x be a random variable form of the distribution with parameters and defined (1) and (2) using the logit of beta by Jones (2004), we then have

$$f_{LWW}^{(x)} = \frac{1}{B(a,b)} [F(x)]^{a-1} [1-F(x)]^{b-1} f(x) \quad (3)$$

Both probability density and cumulative density function (pdf and cdf) of Lehmann Type II weighted Weibull distribution is obtained by substituting pdf and cdf of weighted Weibull distribution in Equations (1) and (2) into Equation (3) and set $a = \lambda = 1$, we then obtain

$$g_{LWWD}^{(x)} = b\left[1-\frac{\alpha+1}{\alpha}\{\left(1-e^{-x^\beta}\right)-\frac{1}{\alpha+1}\left(1-e^{-(1+\alpha)x^\beta}\right)\}\right]^{b-1} \times \frac{\alpha+1}{\alpha}\beta x^{\beta-1}e^{-x^\beta}\left(1-e^{-\alpha x^\beta}\right) \quad (4)$$

Where, $a = 1, b > 0, \lambda = 1, \beta > 0, \alpha > 0 \text{ and } x > 0 \text{ such that } x \sim LWWD(1,b,1,\alpha,\beta)$. Equation (5) is the pdf of Lehmann Type II weighted Weibull distribution.

setting $w(x) = \frac{\alpha+1}{\alpha}\{\left(1-e^{-x^\beta}\right)-\frac{1}{\alpha+1}\left(1-e^{-(1+\alpha)x^\beta}\right)\}$ (5)

$$\frac{\partial w}{\partial x} = \frac{\alpha+1}{\alpha}\beta x^{\beta-1}e^{-x^\beta}\left(1-e^{-\alpha x^\beta}\right)\frac{\alpha+1}{\alpha}\{\left(1-e^{-x^\beta}\right)-\frac{1}{\alpha+1}\left(1-e^{-(1+\alpha)x^\beta}\right)\}$$

substituting dbx into Equation (4), we get

$$g_{LWWD}^{(x)} = b\left[1-\frac{\alpha+1}{\alpha}\{\left(1-e^{-x^\beta}\right)-\frac{1}{\alpha+1}\left(1-e^{-(1+\alpha)x^\beta}\right)\}\right]^{b-1} dw$$

$$w = \frac{\alpha+1}{\alpha}\{\left(1-e^{-x^\beta}\right)-\frac{1}{\alpha+1}\left(1-e^{-(1+\alpha)x^\beta}\right)\} \quad (6)$$

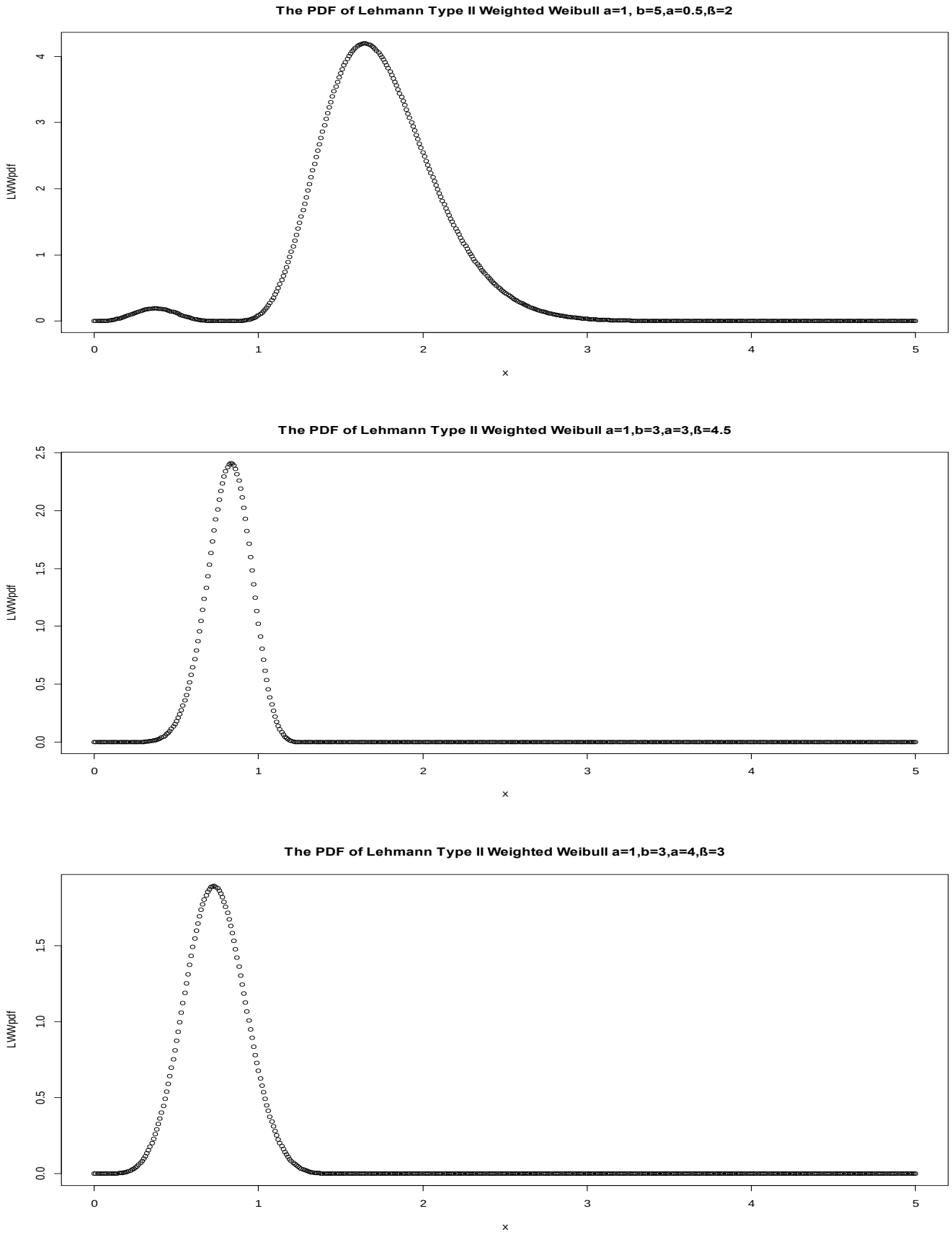

Figure 2. The pdf of LWW distribution at various values of the parameters and it is clear that indeed it is rightly skewed.

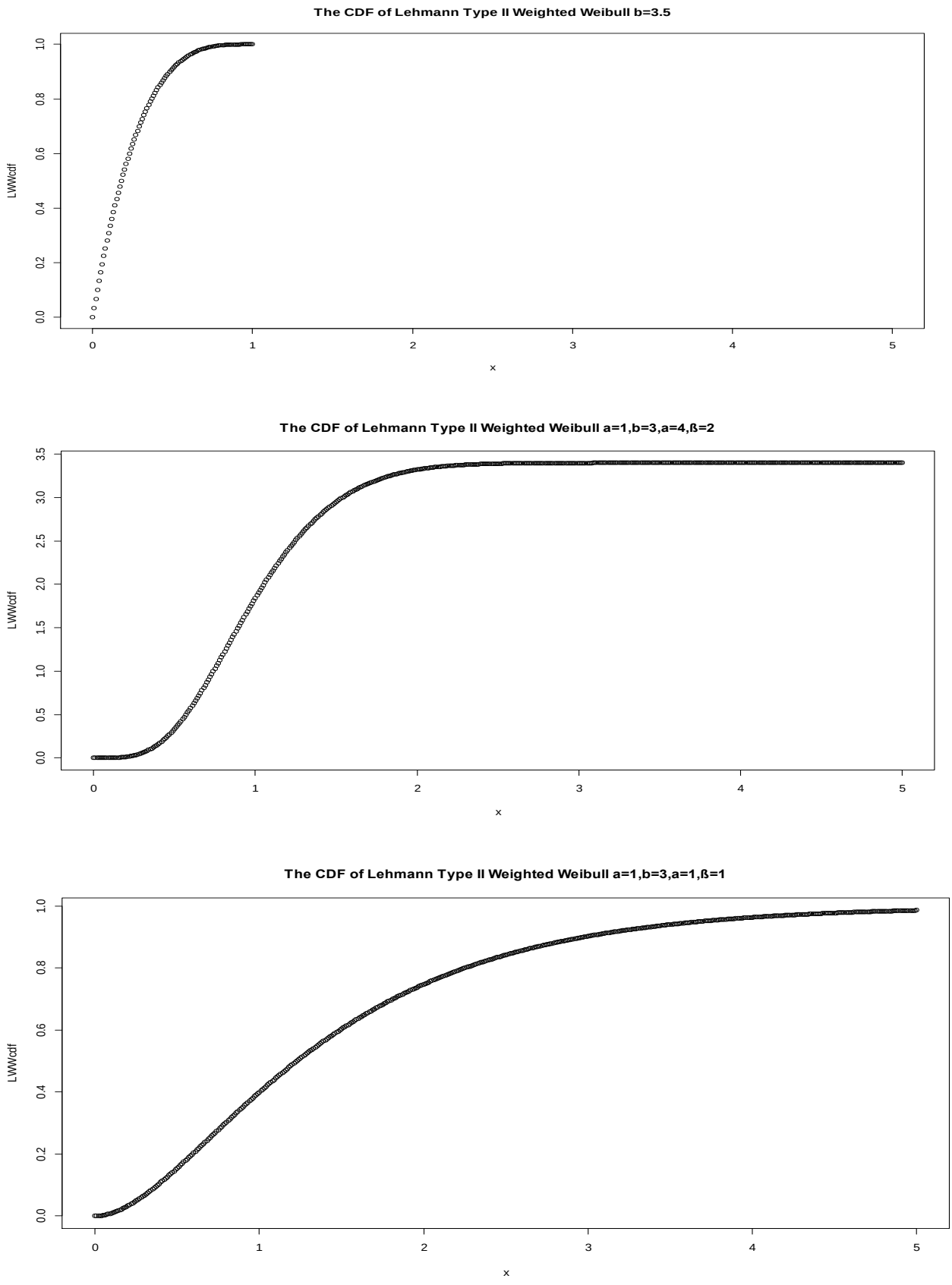

Figure 3. The CDF of LWW with a=1, b=3, $\alpha = 1, \beta = 1$. However, at given various values of the parameters, the graphs give the same pattern and shape.

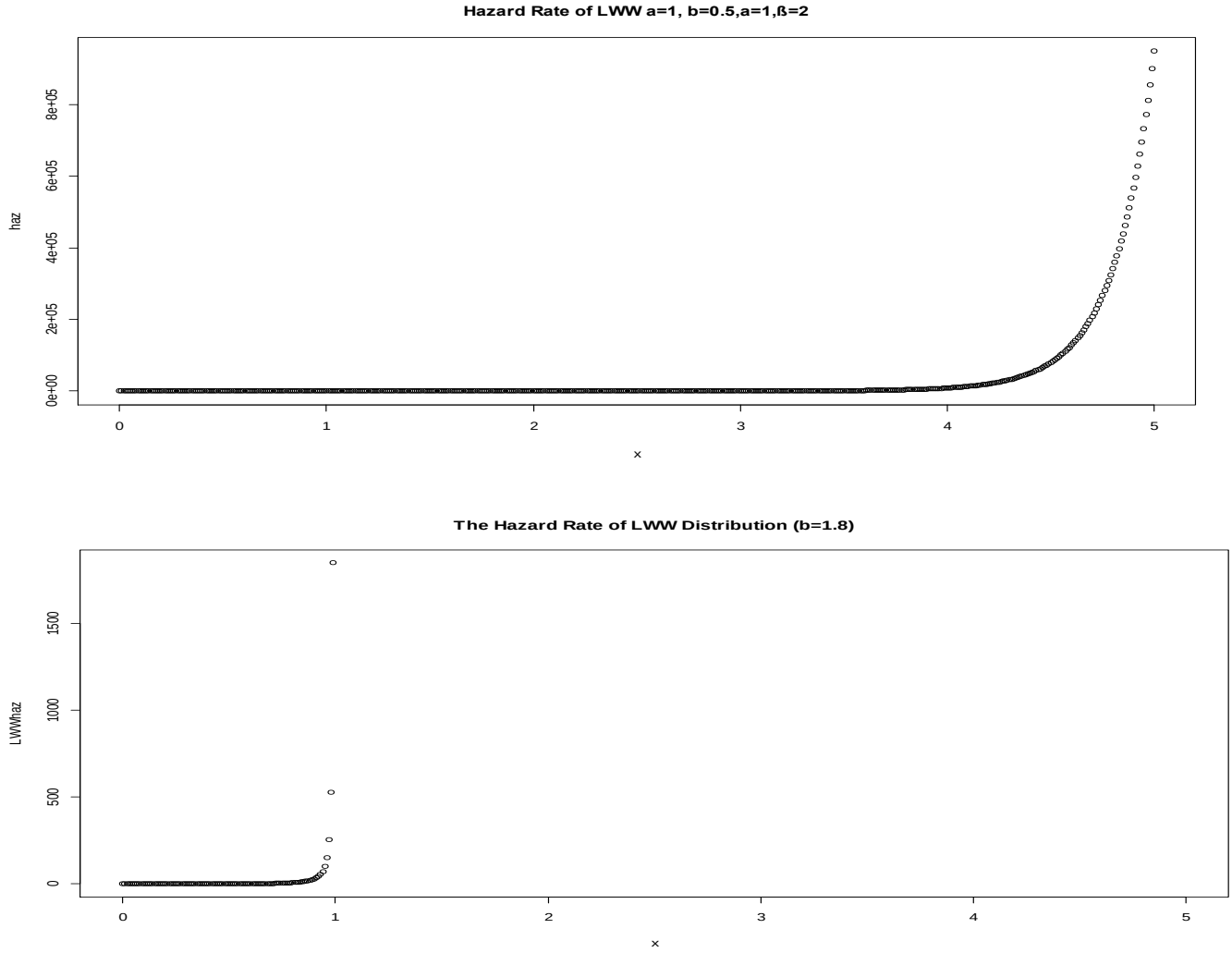

Figure 4. The hazard rate function of Lehmann Type II weighted Weibull distribution with several values of the parameter.

Therefore, Equation (4) can be re-written as

$$g_{LWW}^{(x)} = b[1-W]^{b-1}\frac{dw}{dx} \quad (7)$$

From logit of beta link function, we show that Equation (7) equal to one

$$g_{LWWD}^{(x)} = b\left[1-\frac{\alpha+1}{\alpha}\{\left(1-e^{-x^{\beta}}\right)-\frac{1}{\alpha+1}\left(1-e^{-(1+\alpha)x^{\beta}}\right)\}\right]^{b-1} \times \frac{\alpha+1}{\alpha}\beta x^{\beta-1}e^{-x^{\beta}}\left(1-e^{-\alpha x^{\beta}}\right)$$

Then, recall that $w = \frac{\alpha+1}{\alpha}\{\left(1-e^{-x^{\beta}}\right)-\frac{1}{\alpha+1}\left(1-e^{-(1+\alpha)x^{\beta}}\right)\}$ and using the differential equation method on $\frac{\partial w}{\partial x}$. Therefore, we have

$$b\int_0^1 (1-w)^{b-1}\,dw = 1$$

Figure 2 show the graph of the Lehmann Type II weighted Weibull distribution at different values of the parameters.

Cumulative density function (CDF)

We have defined the probability density function (pdf) of $LWWD(1,b,1,\alpha,\beta)$ in Equation (6), then Equation (6) can be given as

$$G_{LWWD}^{(x)} = P(X \le x) = \int_0^x f(w)\,dw$$

$$= \int_0^x b\left[1-\frac{\alpha+1}{\alpha}\{\left(1-e^{-x^{\beta}}\right)-\frac{1}{\alpha+1}\left(1-e^{-(1+\alpha)x^{\beta}}\right)\}\right]^{b-1}\frac{\alpha+1}{\alpha}\beta x^{\beta-1}e^{-x^{\beta}}\left(1-e^{-\alpha x^{\beta}}\right)\,dw \quad (8)$$

$$G_{LWWD}^{(x)} = P(X \le x) = \int_0^x b[1-W]^{b-1}\,dw$$

$= b\int_0^x [1-W]^{b-1}\,dw$ and cdf is given as

$$G_{LWWD}^{(x)} = [1-(1-x)^{b}] \quad (9)$$

The graph of cumulative distribution of Lehmann Type II Weighted Weibull is shown Figure 3.

The survival rate function

The survival rate function of the $LWWD\,(1, b, 1, \alpha, \beta)$ is defined by

$$S_{LWWD}(x) = 1 - G_{LWWD}(x) = 1 - \int_0^x f(w)dw$$
$$= 1 - b\int_0^x [1 - W]^{b-1}\, dw$$
$$S_{LWWD}(x) = (1 - x)^b \qquad (10)$$

The hazard rate function

The hazard rate function of a random variable x with the pdf and cdf is given by

$$h_{LWWD}(x) = \frac{g_{LWWD}(x)}{1 - G_{LWWD}(x)}$$

However, $LWWD\,(1, b, 1, \alpha, \beta)$ with $g_{LWWD}(x)$ and $G_{LWWD}(x)$ respectively defined in Equations (4) and (9), the hazard rate function can be expressed as:

$$= \frac{b(1-w)^{b-1}w'}{1-[1-(1-x)^b]} \quad \text{or} \quad = \frac{b(1-w)^{b-1}w'}{1 - G_{LWWD}(x)} \qquad (11)$$

Where W is the expression in Equation (5)

To show that $\lim_{x\to\infty} h_{LWWD}(x) = 0$ *and* $\lim_{x\to 0} h_{LWWD}(x) = 0$, we get the following

$$\lim_{x\to\infty} h_{LWWD}(x) = \lim_{x\to\infty} \frac{b(1-w)^{b-1}w'}{1-[1-(1-x)^b]}$$

where, $w' = \frac{\alpha+1}{\alpha}\left\{\left(1 - e^{-x^\beta}\right) - \frac{1}{\alpha+1}\left(1 - e^{-(1+\alpha)x^\beta}\right)\right\}$

=x

$$\lim_{\to\infty} \frac{b\left[1-\frac{\alpha+1}{\alpha}\left\{\left(1-e^{-x^\beta}\right)-\frac{1}{\alpha+1}\left(1-e^{-(1+\alpha)x^\beta}\right)\right\}\right]^{b-1}\frac{\alpha+1}{\alpha}\beta x^{\beta-1}e^{-x^\beta}\left(1-e^{-\alpha x^\beta}\right)}{1-[1-(1-x)^b]}$$

For simplification, we take the limit of the following:

When $x \to \infty = 0$ *and* $x \to 0 = 0$

$$= \lim_{x\to\infty} \frac{\alpha+1}{\alpha}\beta x^{\beta-1}e^{-x^\beta}\left(1 - e^{-\alpha x^\beta}\right) \quad = \lim_{x\to\infty} \frac{\alpha+1}{\alpha}\lambda\beta\infty^{\beta-1}e^{-\infty^\beta}\left(1 - e^{-\alpha\infty^\beta}\right)$$

$$= 0$$

$$= \lim_{x\to 0} \frac{\alpha+1}{\alpha}\beta 0^{\beta-1}e^{-0^\beta}\left(1 - e^{-\alpha 0^\beta}\right) = 0$$

$As\ x \to \infty = 0\ and\ x \to 0 = 0$, Equation (11) above tends to $\infty\ and\ 0$ and equal to zero (Figure 4).

Asymptotic behaviours

Following the steps in "Hazard Rate Function" above, by taking the $\lim_{x\to\infty} g_{LWWD}(x)$ *and* $\lim_{x\to 0} g_{LWWD}(x)$ of the $LWWD\,(1, b, 1, \alpha, \beta)$ distribution which is investigated as follows. Now from Expression (4), we have

$$\lim_{x\to\infty} g_{LWWD}(x) = b\left[1 - \frac{\alpha+1}{\alpha}\left\{\left(1 - e^{-x^\beta}\right) - \frac{1}{\alpha+1}\left(1 - e^{-(1+\alpha)x^\beta}\right)\right\}\right]^{b-1}$$
$$\frac{\alpha+1}{\alpha}\beta x^{\beta-1}e^{-x^\beta}\left(1 - e^{-\alpha x^\beta}\right)$$

taking the limit

$$= \lim_{x\to\infty} \frac{\alpha+1}{\alpha}\beta x^{\beta-1}e^{-x^\beta}\left(1 - e^{-\alpha x^\beta}\right)$$
$$= \lim_{x\to\infty} \frac{\alpha+1}{\alpha}\beta\infty^{\beta-1}e^{-\infty^\beta}\left(1 - e^{-\alpha\infty^\beta}\right) = 0$$
$$= \lim_{x\to 0} \frac{\alpha+1}{\alpha}\beta 0^{\beta-1}e^{-0^\beta}\left(1 - e^{-\alpha 0^\beta}\right) \quad = 0$$

This shows that the asymptotic behaviours when $x \to \infty = 0\ and\ x \to 0 = 0$, and it is sure that the distribution has at least a mode.

MOMENTS AND MOMENT GENERATING FUNCTION

Shittu and Adepoju (2013) described that when a random variable following a generalized beta generated distribution that is, $x \sim GBG(f, 1, b, c)\ then\ \mu_r' = E[F^{-1}\cup^{\frac{1}{c}}]^r$ where $\cup \sim B(1, b), c$ is a constant and $F^{-1}(x)$ is the inverse of CDF of the weighted Weibull distribution, since $LWWD\,(1, b, 1, \alpha, \beta)$ distribution is a special form when a=c=1.We then derive the moment generating function (mgf) of the proposed distribution $m(t) = E(e^{tx})$ and the general rth moment of a beta generated distribution is defined by

$$\mu_r' = b\int_0^1 [F^{-1}(x)]^r\,[1 - x]^{b-1}\, dx \qquad (12)$$

Also, using the taylor series expansion around the point $E(x_f) = \mu_f$ to obtain

$$\mu_r' = \sum_{u=0}^{r}\binom{r}{u}[F^{-1}(\mu)]^{r-u}\,[F^{-1(1)}(\mu_f)]^u \sum_{u=0}^{n}(-1)^i\binom{r}{i} \qquad (13)$$

Cordeiro et al. (2011) described an alternative series expansion in their paper for μ_r' in terms of $r(r, z) = E(Z^r\,F(Z)^Y)$ where k follows the parent distribution then for z = 0, 1, …

$$\mu_r' = b\sum_{i=0}^{\infty}(-1)^i\binom{b-1}{i}\,r(r, i-1)$$

They further discussed another mgf of x for generated beta distribution

$$M(t) = b\sum_{i=0}^{\infty}(-1)^i\binom{b-1}{i}\rho(t, i-1) \qquad (14)$$

Where, $\rho(t,\ r) = \int_{-\infty}^{\infty} e^{tx}[F(x)]^m\, f(x)\, dx$

Therefore,

$$M_x^{(t)} = b\sum_{i=0}^{\infty}(-1)^i\binom{b-1}{i}\int_{-\infty}^{\infty} e^{tx}[F(x)]^{(i+1)-1}\, f(x)\, dx \qquad (15)$$

Substituting both pdf and cdf (F(x) and f(x)) of the weighted Weibull distribution into Equation (15), we obtain

$$M_{LWWD(x)}^{(t)} = b\sum_{i=0}^{\infty}(-1)^i\binom{b-1}{i}\int e^{tx}\left[\frac{\alpha+1}{\alpha}\left\{\left(1-e^{-x^\beta}\right)-\frac{1}{\alpha+1}\left(1-e^{-(1+\alpha)x^\beta}\right)\right\}\right]^{(i+1)-1} \times \frac{\alpha+1}{\alpha}\beta x^{\beta-1}e^{-x^\beta}\left(1-e^{-\alpha x^\beta}\right)dx \quad (16)$$

Equation (17) becomes the mgf of Lehmann Type II weighted Weibull distribution and by setting b=1 and i = 0, the same expression (17) is reduced to become the parent distribution. To obtain the rth moment of $LWWD(1,b,1,\alpha,\beta)$, the weighted Weibull distribution by Shahbaz et al. (2010) is given by

$$M_{(x)}^{(t)} = \int_0^{\infty} e^{tx}\frac{\alpha+1}{\alpha}\beta x^{\beta-1}e^{-x^\beta}(1-e^{-\alpha x^\beta})\,dx$$

$$= \sum_{j=0}^{\infty}\frac{t^j}{j!\alpha^\beta}\{1+\alpha-(1+\alpha)^{-\frac{j}{\beta}}\}\Gamma(1+\frac{j}{\beta}) \quad (17)$$

Equation (16) can be re-written as

$$M_{LWWD(x)}^{(t)} = b\sum_{i=0}^{\infty}\sum_{j=0}^{\infty}(-1)^i\binom{b-1}{i}\frac{t^j}{j!\alpha^\beta}\{1+\alpha-(1+\alpha)^{-\frac{j}{\beta}}\}\Gamma(1+\frac{j}{\beta})\} \quad (18)$$

Moreover, the rth moment of the proposed distribution can also be written from the above equation (18) as given below:

$$\mu'_{LWWD(r)} = E(X^r) =$$

$$b\sum_{i=0}^{\infty}(-1)^i\binom{b-1}{i}\frac{t^r}{r!\alpha^\beta}\{1+\alpha-(1+\alpha)^{-\frac{j}{\beta}}\}\Gamma(1+\frac{j}{\beta})\} \quad (19)$$

Again, setting b = 1 in Equation (19) leads to the rth moment of the weighted Weibull distribution by Shahbaz et al. (2010) and is given by

$$\mu'_r = E(X^r) = \frac{r}{\alpha}\{1+\alpha-(1+\alpha)^{-\frac{j}{\beta}}\}\Gamma(1+\frac{j}{\beta})\}$$

While the rth moment of the proposed distribution is

$$\mu'_{LWWD(r)} = E(X^r) =$$

$$b\sum_{i=0}^{\infty}(-1)^i\binom{b-1}{i}\frac{r}{\alpha}\{1+\alpha-(1+\alpha)^{-\frac{j}{\beta}}\}\Gamma(1+\frac{j}{\beta})\} \quad (20)$$

From Equation (20), one can easily obtain the mean about the origin e.g when r = 1and the second moment when r = 2, etc. The first moment of $LWW(1,b,\lambda,\beta,\alpha)$ is obtain

$$\mu'_{LWWD(1)} = E(1,b,\alpha,\beta)^{(x)} = E(X') = b\sum_{i=0}^{\infty}(-1)^i\binom{b-1}{i}\frac{1}{\alpha}\{1+\alpha-(1+\alpha)^{-\frac{1}{\beta}}\}\Gamma(1+\frac{1}{\beta}) \quad (21)$$

The second moment can also be obtained as follows:

$$\mu'_{LWWD(2)} = V(1,b,\alpha,\beta)^{(x)} = K_1 - K_2 \quad (22)$$

where,

$$K_1 = E(1,b,\lambda,\beta,\alpha)^{(X^2)} = b\sum_{i=0}^{\infty}(-1)^i\binom{b-1}{i}\frac{2}{\alpha}\{1+\alpha-(1+\alpha)^{-\frac{2}{\beta}}\}\Gamma(1+\frac{2}{\beta})$$

$$K_2 = E(1,b,\lambda,\beta,\alpha)^{(X)} = b\sum_{i=0}^{\infty}(-1)^i\binom{b-1}{i}[\frac{1}{\alpha}\{1+\alpha-(1+\alpha)^{-\frac{1}{\beta}}\}\Gamma(1+\frac{1}{\beta})]^2$$

We can also get the standard deviation (SD) as

$$SD_{LWWD}(1,b,\alpha,\beta)\ \ (X) = \sqrt{K_1-K_2} \quad (23)$$

Others like coefficient of variation, skewness and kurtosis can easily be obtained.

ESTIMATION OF PARAMETER

The maximum likelihood estimate (MLEs) of the parameter of $LWWD(1,b,\alpha,\beta)$ distribution following Cordeiro et al (2011) given the log-likelihood function for $\tau = (1,b,c,\theta)$, where $\theta = (\alpha,\beta)$. Shittu and Adepoju (2013) in their study discussed that by setting τ to be a vector of parameter and given by

$$L(\tau) = nlogc - nlogb + \sum_{i=1}^{n}\log[f(x;\theta)] + (b-1)\sum_{i=1}^{n}\log[1-F(x;\theta)] \quad (24)$$

Recall that, a = c = 1 (24) becomes $\tau = (1,b,1,\theta)$

$$L(\tau) = -nlog(b) + \sum_{i=1}^{n}\log[f(x;\theta)] + (b-1)\sum_{i=1}^{n}\log[1-F(x;\theta)] \quad (25)$$

where, $f(x;\theta) = \frac{\alpha+1}{\alpha}\beta x^{\beta-1}e^{-x^\beta}\left(1-e^{-\alpha x^\beta}\right)$ and

$$F(x;\theta) = \frac{\alpha+1}{\alpha}\left\{\left(1-e^{-x^\beta}\right)-\frac{1}{\alpha+1}\left(1-e^{-(1+\alpha)x^\beta}\right)\right\}$$

$$L_{LWWD}^{(\tau)} = -nlog(b) + \sum_{i=1}^{n}\log\left[\frac{\alpha+1}{\alpha}\beta x^{\beta-1}e^{-x^\beta}\left(1-e^{-\alpha x^\beta}\right)\right] + (b-1)\sum_{i=1}^{n}\log[1-\frac{\alpha+1}{\alpha}\left\{\left(1-e^{-x^\beta}\right)-\frac{1}{\alpha+1}\left(1-e^{-(1+\alpha)x^\beta}\right)\right\}] \quad (26)$$

For determining the MLE of b,β,α, we took the partial derivative of Equation (26) with respect to (b,β,α) as follows:

$$\frac{L_{LWWD}^{(\tau)}}{\partial b} = -nlog(1,b) + (b-1)\sum_{x=1}^{n}\log[1-\frac{\alpha+1}{\alpha}\left\{\left(1-e^{-x^\beta}\right)-\frac{1}{\alpha+1}\left(1-e^{-(1+\alpha)x^\beta}\right)\right\}] \quad (27)$$

$$\frac{L_{LWWD}^{(\tau)}}{\partial\alpha} = \sum_{x=1}^{n}log\left[\frac{\frac{\partial}{\partial\alpha}\frac{\alpha+1}{\alpha}\beta x^{\beta-1}e^{-x^\beta}\left(1-e^{-\alpha x^\beta}\right)}{\frac{\alpha+1}{\alpha}\beta x^{\beta-1}e^{-x^\beta}\left(1-e^{-\alpha x^\beta}\right)}\right] + (b-1)\sum_{x=1}^{n}\log\left[\frac{\frac{\partial}{\partial\alpha}(1-\frac{\alpha+1}{\alpha}\left\{\left(1-e^{-x^\beta}\right)-\frac{1}{\alpha+1}\left(1-e^{-(1+\alpha)x^\beta}\right)\right\})}{1-\frac{\alpha+1}{\alpha}\left\{\left(1-e^{-x^\beta}\right)-\frac{1}{\alpha+1}\left(1-e^{-(1+\alpha)x^\beta}\right)\right\}}\right] \quad (28)$$

$$\frac{L_{LWWD}^{(\theta)}}{\partial\beta} = \sum_{x=1}^{n}log\left[\frac{\frac{\partial}{\partial\beta}\left[\frac{\alpha+1}{\alpha}\beta x^{\beta-1}e^{-x^\beta}\left(1-e^{-\alpha x^\beta}\right)\right]}{\frac{\alpha+1}{\alpha}\beta x^{\beta-1}e^{-x^\beta}\left(1-e^{-\alpha x^\beta}\right)}\right] + (b-1)\sum_{x=1}^{n}\log\left[\frac{\frac{\partial}{\partial\beta}(1-\frac{\alpha+1}{\alpha}\left\{\left(1-e^{-x^\beta}\right)-\frac{1}{\alpha+1}\left(1-e^{-(1+\alpha)x^\beta}\right)\right\})}{1-\frac{\alpha+1}{\alpha}\left\{\left(1-e^{-x^\beta}\right)-\frac{1}{\alpha+1}\left(1-e^{-(1+\alpha)x^\beta}\right)\right\}}\right] \quad (29)$$

The above equations can be solved using Newton Ralphson method to obtain the $\hat{b},\hat{\alpha},\hat{\beta}$ the MLE of (b,α,β) respectively.

Taking second derivatives of Equations 27, 28 and 29 with respect to the parameters above we can derive the interval estimate and hypothesis tests on the model parameter and inverse of fisher's information matrix needed.

RESULTS AND DISCUSSION

Application to life time data set

Here we used a data set studied by Shahbaz et al (2010) on life components in years to compare the Lehmann Type II weighted Weibull and weighted Weibull distribution. The data contains Life (Grouped data say (0 – 1.0, 1.0 – 2.0,…,> 5.0) and frequency all together is 123619. R software is used to determine the maximum likelihood estimates and the log-likelihood for the Lehmann Type II weighted Weibull distribution are: $\hat{b} = 7.90434,\ \hat{\beta} = 8.44282,\ \hat{\alpha} = 8.70033\ and\ l_{g_{LWW}} = 454.4$ while the maximum likelihood estimates and the log-likelihood for the weighted Weibull distribution are: $\hat{\beta} = 8.649918,\ \hat{\alpha} = 8.041522$ and $l_{g_{WW}} = 452.4337$, where $l_{g_{LWW}}\ and\ l_{g_{WW}}$ denote log-likelihood of both Lehmann Type II weighted Weibull distribution and weighted Weibull distribution. The asymptotic covariance matrix of the maximum likelihood estimates for the Lehmann Type II weighted Weibull distribution, which is generated from the inverse of fisher's information matrix and is given by

$$\begin{pmatrix} 0.4754645 & 0.0000000 & 0.0000000 \\ 0.0000000 & 0.5330965 & 0.0000000 \\ 0.0000000 & 0.0000000 & 0.5674899 \end{pmatrix}$$

Following the result above, this shows that the new proposed distribution can take care even more skew data than the weighted Weibull distribution because of the additional shape parameter b, and with the hope that the model will be wider application to many areas of research e.g economics, finance, environmental, biomedical among others.

Conclusion

In a nut shell, we studied the statistical properties of the proposed distribution e.g moments, moment generating function, estimation of parameters with R software are presented in this paper. We also upgraded with an additional parameter to the existing two parameters in the weighted Weibull distribution and with the method of maximum likelihood the parameters of the model were estimated in order to give way for the derivation of fisher information matrix. The data used indicates that Lehmann Type II weighted Weibull distribution has a better representation of data and more flexible than weighted Weibull distribution.

Conflict of Interests

The author(s) have not declared any conflict of interests.

REFERENCES

Azzalini A (1985). A class of distributions which include the normal ones, Scand. J. Stat. 12:171-178.
Shahbaz S, Shahbaz MQ, Butt NZ (2010). A class of weighted Weibull distribution in Pakistan J. Statistics Operation Res. VI(1):53-59.
Cordeiro GM, Alexandra C, Ortega MM, Edwin Sarabia JM (2011). Generalized Beta Generated distributions. ICMA Centre. Discussion Papers in Finance DP 2011-05. pp. 1-29.
Gupta RD, Kundu D (1990). The role of weighted distribution in stochastic modeling. Communications in statistics, 19:3147-3162.
Eugene NC, Famoye F (2002). Beta-Normal distribution and its applications. Communications in Statistics – Theory and Methods 31:497-512.
Famoye F, Lee C, Olugbenga O (2005). The beta-Weibull distribution. J. Statistical Theory Applications, 4(2):121-138.
Jones MC (2004). Families of distributions arising from distributions of order statistics test 13:1-43.
Lee C, Famoye F, Olumolade O (2007). Beta-Weibull distribution: Some properties and applications to censored data. J. modern Appl. statistical methods, 6:173-186.
Nadarajah S, Kotz S (2005). The beta exponential distribution. Reliability Eng. Syst. Safety, 91:689-697.
Shittu OI, Adepoju AK (2013). On the Beta-Nakagami Distribution. Progress in Appl. Maths. 5(1):49-58.

academicJournals

Vol. 9(4), pp. 79-81, 28 February, 2014
DOI: 10.5897/IJPS2013.4094
ISSN 1992 - 1950

http://www.academicjournals.org/IJPS

International Journal of Physical Sciences

Short Communication

Metamaterials in microwave applications: A selective survey

Vipul Sharma[1]*, S. S. Pattnaik[2] and Tanuj Garg[1]

[1]Department of Electronics and Communication Engineering, Gurukul Kangri University, Haridwar, India.
[2]Department of ETV, NITTTR, Chandigarh, India.

Received 17 December, 2013; Accepted 27 January, 2014

Recently, metamaterial has grabbed prime focus of research fraternity working in the field of antennas, microwave filters and components design. Many different structures of split ring resonators (SRR) for their respective applications have been reported till date. In all of these findings in some way or other, using metamaterial, drastic reduction in size of the component has been achieved. Thus, the metamaterial can be viewed as a powerful miniaturization tool in the field of radio frequency (RF) and microwave. Since its inception in 1999, many variants of SRR have come up leading to more efficient designs with better RF properties. This review paper presents an application based review of such variants and will be useful for new researchers exploring its use in their research problems.

Key words: Metamaterial, antenna miniaturization, negative refractive index metamaterial (NRIM),split ring resonators (SRR).

INTRODUCTION

In a pioneering paper, written in 1968, Prof. V.G. Vaselego coined a term Metamaterial, a hypothetical material having negative value of electrical and magnetic permeabilities and theoretically he derived the properties (Vaselego, 1968). For almost thirty years after its inception, there was hardly any substantial work reported this field. In 1999, Pendry et al. first realized negative permeability by introducing periodic array of nonmagnetic conducting units. They demonstrated that periodic array of nonmagnetic conductor split rings show negative effective permeability at high frequency side of resonance (Pendry et al., 1999). It was first time in year 2000, when Smith et al. came up with physical realization of simultaneously negative values of effective magnetic permeability and electrical permittivity and thus a negative value of refractive index (NRIM) in microwave regime (Smith et al., 2000). The structure they called left handed medium comprised of periodic array of interspaced conducting nonmagnetic split ring resonators and continuous wires. The array conducting wire provided electric field resonance and thus negative value of electrical permittivity. Since then many variants of split ring structure have been reported by researchers for different engineering applications. But complete potential of metamaterial is yet to be explored. The main objective of this review paper is to discuss different variants of metamaterial structure and their applicability in microwave engineering problems.

METAMATERIALS IN MICROWAVE APPLICATIONS

Metamaterial in the form of various structures has been extensively used by the microwave researchers to design

*Corresponding author. E-mail: vipul.s@rediffmail.com

miniaturized microwave components, filters and antennas. Sabah et al. (2010) presented a method of mechanical tuning of metamaterial resonant frequency by varying substrate thickness. In the paper, a metamaterial structures whose unit cell has triangular split ring resonator (TSRR) and wire strip (WS) have been analyzed for S- and C- microwave bands. Retrieval method has been used for calculation of effective material parameters. Simulation results show that the new metamaterials exhibits double negative properties in the frequency region of interest and their resonant frequency can be tuned by varying substrate thickness. In Sulaiman et al. (2010), the authors proposed two types of metamaterial composed of patch antennas, one antenna using metamaterial as substrate and the other one using metamaterial as cover. Perfectly electric conductor in omega shape on RT 5880 substrate has been used as metamaterial unit. When metamaterial unit is used as substrate of patch antenna, there exist drastic reduction in size of the patch, and becomes comparable to the metamaterial unit. The reduction in size is also accompanied by improvement in return loss. The price paid is the bandwidth. This antenna is found suitable for narrow band applications. When planar array slab consisting of metamaterial units is used as a cover of conventional patch antenna, significant improvement in directivity was also observed.

In Ziolkowski et al. (2009), the authors present design, fabrication and simulation of electrically small, coaxially fed metamaterial inspired Z antennas having ability to change resonant frequency by changing value of lumped element inductor. The structure consists of a coaxially fed monopole printed on one side of RT5880 substrate, while Z element printed on the other side. The Z element is composed by joining two “J” elements connected by a lumped element inductor. The authors have tested the design for two Z-antennas one at 570 MHz and another at 300 MHz. The results show that by changing value of lumped element inductor joining the two “J” elements, the resonant frequency of the antenna can be successfully changed.

Further, Palandoken et al. (2009) also presented a novel application of metamaterial for antenna miniaturization. Metamaterial is composed of unit cells having spiral rings connected to metal strips on both sides of FR4 substrate, arranged in 2×3 planar array form. The antenna comprises of a printed dipole directly connected to three of six unit cells. Rectangular slot in truncated ground plane allows better impedance matching. It has been shown that loaded dipole gives broad bandwidth about 63% with drastic reduction in size.

Ziolkowski et al. (2009) also explored the metamaterial property to design antenna at 300 MHz. This paper demonstrates electrically small, metamaterial inspired 3D magnetic EZ antenna, consisting of extruded capacitively loaded loop (CLL) driven by coaxially fed semi loop antenna. Resonant frequency of the antenna is found tunable by amount of Quartz filled capacitive gap of CLL) element. The antenna is found to be nearly matched without any external circuit and shows more than 95% efficiency with a fractional bandwidth of 1.66%. Sharma et al. (2011) introduced elliptical split ring resonator (ESRR structure to get metamaterial property. The structure is dual fed in offset and shows negative value refractive index at multiple frequencies. When tested for radiation properties the ESRR gives highly directional radiation pattern. In the design of metamaterial antennas some researchers also addressed the issue of optimization in design. Vidyalakshmi et al. (2009) proposed a hybrid of genetic algorithm (GA) and artificial neural network (ANN) called GA ANN for optimization of metamaterial split ring resonator to achieve given resonant frequency. Size of outer square ring, conductor width, dielectric spacing between outer and inner rings are inputs to the optimization program and error between desired resonant frequency and calculated resonant frequency has been taken as cost function to be minimized. ANN has been used to obtain fitness of chromosomes. Performance GA ANN when compared with stand alone GA and stand alone ANN, GA ANN converges more fast and gives higher accuracy. Sumanta et al. (2012) introduced a new structure, N-sided Regular Polygon Split Ring Resonator (NRPSRR). They have also nicely presented the mathematical analysis and derivation of the structure. Further my increasing the limit of N to infinity, they have obtained resonant frequency for cicular SRR. Genetic Algorithm has been successfully used to obtain simulation model of the structure.

Conclusion

The paper presents a selective review of findings reported by various researchers in the field of metamaterial research and its application in microwave structures. Various microwave structures using metamaterial for miniaturization, have been discussed. Mathematical modelling of metamaterial is a new dimension; the research fraternity is focussing now. Less research has been reported in this particular field till date. The aspect has been addressed in this survey. This paper will go a long way for the new scientists interested to use metamaterial in microwave application and miniaturization problems.

Conflict of Interests

The author(s) have not declared any conflict of interests.

REFERENCES

Palandoken M, Grede A, Heino H (2009). Broadband Microstrip Antenna With Left-Handed Metamaterials”, IEEE Trans. Ant. Prop. 57(2):331-338.

Pendry JB, Holden AJ, Robbins DJ, Stewart WJ (1999). Magnetism

from conductors and enhanced nonlinear phenomena. IEEE Trans. Microwave Theory Technique, 47:2075–2084.
Sabah C (2010). Tunable Metamaterial Design Composed of Triangular Split Ring Resonator and Wire Strip for S- and C- Microwave bands", PIER B 22:341-357.
Smith DR Padilla Willie J, Vier DC, Nemat-Nasser SC, Schultz S (2000). Composite Medium with Simultaneously Negative Permeability and Permittivity, Phys. Rev. Lett. 84(18):4184-4187.
Sulaiman AA, Othman A, Jusoh MH, Baba NH, Awang RA, Ain MF (2010). Small Patch Antenna on Omega Structure Metamaterial. Europ. J. Sci. Res. 43(4):527-537.
Sumanta Bose M. Ramaraj Dr. S (2012). Raghavan, Swadhyaya Kumar, Mathematical Modeling, Equivalent Circuit Analysis and Genetic Algorithm Optimization of an N-sided Regular Polygon Split Ring Resonator (NRPSRR), 2nd International Conference on Communication, Computing. Security [ICCCS], Procedia Technology 6:763-770.
Vidyalakshmi MR, Raghavan S (2010). Comparison of Optimization Techniques for Square Split Ring Resonator, Int. J. Microwave. Optical Technol. 5(5):280-286.
Ziolkowski RW, Jin P, Nielsen JA, Tanielian MH, Holloway CL (2009). Experimental Verification of Z Antennas at UHF Frequencies", IEEE Antenna and Wireless Propagation Lett. 8:1329-1333.
Ziolkowski RW, Lin CC, Nielson ja, Tanielian MH, Holloway CL (2009). Design and Experimentation Verification of a 3D Magnetic EZ Antenna at 300 MHz", IEEE Ant Wireless Prop Letters. P. 8.

academicJournals

Related Journals Published by Academic Journals

■African Journal of Pure and Applied Chemistry

■Journal of Internet and Information Systems

■Journal of Geology and Mining Research

■Journal of Oceanography and Marine Science

■Journal of Environmental Chemistry and Ecotoxicology

■Journal of Petroleum Technology and Alternative Fuels